Significance of nuclear cathepsin V in normal thyroid epithelial and carcinoma cells

Al-Hashimi, A., Venugopalan, V., Sereesongsaeng, N., Tedelind, S., Pinzaru, A. M., Hein, Z., Springer, S., Weber, E., Führer, D., Scott, C. J., Burden, R. E., & Brix, K. (2020). Significance of nuclear cathepsin V in normal thyroid epithelial and carcinoma cells. *Biochimica et Biophysica Acta - Molecular Cell Research*, *1867*(12), Article 118846. https://doi.org/10.1016/j.bbamcr.2020.118846

Published in:
Biochimica et Biophysica Acta - Molecular Cell Research

Document Version:
Peer reviewed version

Significance of nuclear cathepsin V in normal thyroid epithelial and carcinoma cells

Alaa Al-Hashimi [1], Vaishnavi Venugopalan [1], Naphannop Sereesongsaeng [2], Sofia Tedelind [1,3], Alexandra M. Pinzaru [1,4], Zeynep Hein [1], Sebastian Springer [1], Ekkehard Weber [5], Dagmar Führer [6], Christopher J. Scott [7], Roberta E. Burden [2], and Klaudia Brix [1]

[1] Department of Life Sciences and Chemistry, Jacobs University Bremen, Campus Ring 1, 28759 Bremen, Germany

[2] School of Pharmacy, Queen's University Belfast, 97 Lisburn Road, Belfast BT9 7BL, UK

[3] Present Address: Gothenburg, Sweden

[4] Present Address: The Rockefeller University, New York City, New York, USA

[5] Institute of Physiological Chemistry, Martin Luther University Halle-Wittenberg, Hollystrasse 1, D-06114 Halle-Saale, Germany

[6] Universität Duisburg-Essen, Universitätsklinikum Essen (AöR), Klinik für Endokrinologie, Diabetologie und Stoffwechsel, Hufeland Strasse 55, D-45177 Essen, Germany

[7] Patrick G. Johnston Centre for Cancer Research, School of Medicine, Dentistry and Biomedical Sciences, Queen's University Belfast, 97 Lisburn Road, Belfast BT9 7BL, UK

Abstract

Altered expression and/or localization of cysteine cathepsins is believed to involve in thyroid diseases including cancer. Here, we examined the localization of cathepsins B and V in human thyroid tissue sections of different pathological conditions by immunolabeling and morphometry. Cathepsin B was mostly found within endo-lysosomes as expected. In contrast, cathepsin V was detected within nuclei, predominantly in cells of cold nodules, follicular and papillary thyroid carcinoma tissue, while it was less often detected in this unusual localization in hot nodule and goiter tissue. To understand the significance of nuclear cathepsin V in thyroid cells, this study aimed to establish a cellular model of stable nuclear cathepsin V expression. As representative of a specific form lacking the signal peptide and part of the propeptide, N-terminally truncated cathepsin V fused to eGFP recapitulated the nuclear localization of endogenous cathepsin V throughout the cell cycle in Nthy-ori 3-1 cells. Interestingly, the N-terminally truncated cathepsin V-eGFP was more abundant in the nuclei during S phase. These findings suggested a possible contribution of nuclear cathepsin V forms to cell cycle progression. Indeed, we found that N-terminally truncated cathepsin V-eGFP expressing cells were more proliferative than those expressing full-length cathepsin V-eGFP or wild type controls. We conclude that a specific molecular form of cathepsin V localizes to the nucleus of thyroid epithelial and carcinoma cells, where it might involve in deregulated pathways leading to hyperproliferation. These findings highlight the necessity to better understand cathepsin trafficking in health and disease. In particular, cell type specificity of mislocalization of cysteine cathepsins, which otherwise act in a functionally redundant manner, seems to be important to understand their non-canonical roles in cell cycle progression.

(275 words)

Keywords

Cysteine cathepsins, non-canonical trafficking, nuclear forms, proliferation-promoting, thyroid cancer

1. Introduction

Cysteine cathepsins belong to a well-investigated group of proteases, namely, the papain-like family C1 of clan CA [1]. Nowadays, it is accepted that the localization and proteolytic activities of cysteine cathepsins are not restricted to endo-lysosomes, since many studies have demonstrated their presence in the cytosol, the nucleus, the mitochondria and in the extracellular space upon secretion [2, 3]. Besides their essential protein processing and degradation tasks as endo-lysosomes enzymes, cysteine cathepsins are hence involved in many more physiological and pathological processes.

The significance of cysteine cathepsins has been studied by us and others in the thyroid gland under physiological and thyroid hormone (TH) challenging conditions, such as in hypo- and hyperthyroidism, or, when thyroid epithelial cells are lacking TH transporters or other regulatory molecules [4, 5]. Cysteine cathepsins also play a role in thyroid cancer, a notion derived from studying cathepsin B in particular [6-8]. Cathepsin B expression is upregulated and it is secreted toward the extracellular space of thyroid carcinoma cells *in situ*, suggesting an initial contribution of cathepsin B to tumor cell invasiveness and metastasis through excessive degradation of the extracellular matrix [6, 7, 9-11]. However, specific forms of cathepsin B were detected in thyroid carcinoma cell nuclei, where they might be involved in histone processing [8]. Moreover, we observed cathepsin V, but not cathepsin L, to be localized to the nuclei of thyroid carcinoma cells by immunofluorescence studies and by immunoblotting upon subcellular fractionation [8].

Several recent studies highlighted nuclear localization of cysteine cathepsins in many different cell types, both in physiology and pathology, and discussed new roles for these versatile proteases in regulating cell fate decisions [3, 12-16]. Hence, we and others proposed that proteolytic functions of nuclear forms of cysteine cathepsins are involved in the processing of specific nuclear proteins, which in turn might implicate these proteases in the regulation of cell cycle progression. It is important to note that most of the previous studies focused on the ubiquitously expressed cathepsins B and L, whereas only little information exists to date about cathepsin V, the closest relative of cathepsin L [3, 8]. Given the relatedness and functional redundancy of cysteine cathepsins [5, 17], it is important to know which of them acts precisely where and when in a particular cell type or specific cancer. In particular, the precise function of nuclear cysteine cathepsin V in thyroid epithelial and carcinoma

cells [8] is not yet understood in sufficient detail, nor is the molecular nature of cathepsin V forms known that become detectable in a number of different thyroid conditions.

Hence, this study aims to investigate the expression and function of cathepsin V in order to shed light on its roles in thyroid health and disease. Specifically, we investigated whether nuclear cathepsin V is a result of mistrafficking or whether it results from altered protein translation. There are different hypotheses as to how cathepsin V reaches the nucleus of thyroid cells [3]: either the mature active form of cathepsin V leaks out of endo-lysosomes, or there is alternative splicing or leaky scanning resulting in the translation of a specific cathepsin V form at free ribosomes in the cytosol, which would not follow the canonical trafficking pathway along the secretory route because the signal peptide is lacking. Here, we propose such an N-terminally truncated specific form of cathepsin V, which does not bear the ER lumen-targeting signal peptide and lacks part of the propeptide, for its potential nuclear fate. Therefore, we established two cell lines stably expressing full-length and the N-terminally truncated specific form of cathepsin V, both tagged with enhanced green fluorescent protein (eGFP) at their C-termini, in order to test which of the two is possibly reaching the nucleus of thyroid epithelial and/or carcinoma cells. It is important to note that, in contrast to the full-length protease, N-terminally truncated cysteine cathepsin V is indeed targeted for nuclear entry in the newly established cellular models, where it promotes thyrocyte proliferation.

2. Materials and Methods

2.1 Vector construction

A vector encoding human full-length cathepsin B (*p*hCB-eGFP) was designed from the cDNA of cathepsin B obtained from the human keratinocyte cell line HaCaT, which was then inserted into the mammalian expression vector *p*EGFP-N1 (Clontech, Heidelberg, Germany) by using the *Eco*RI and *Bam*HI restriction sites [18]. The *CTSV* open reading frame, originally in *p*cDNA3.1 (GenScript, Leiden, The Netherlands) was subcloned into the *p*EGFP-N1 plasmid using *Eco*RI and *Bam*HI to generate the vector coding for human full-length cathepsin V. Vectors encoding human N-terminally truncated cathepsin B (*p*h52NCB-eGFP) and human N-terminally truncated cathepsin V (*p*h56NCV-eGFP) were each engineered such that upon translation the pre-peptides and parts of the pro-peptides are lacking (Fig. 1). Thus, translation was thought to become initiated at the second start codon corresponding to methionine at positions 52 and 56, respectively, and inserted into the *p*EGFP-N1 vector using the *Xho*I and *Bam*HI restriction sites.

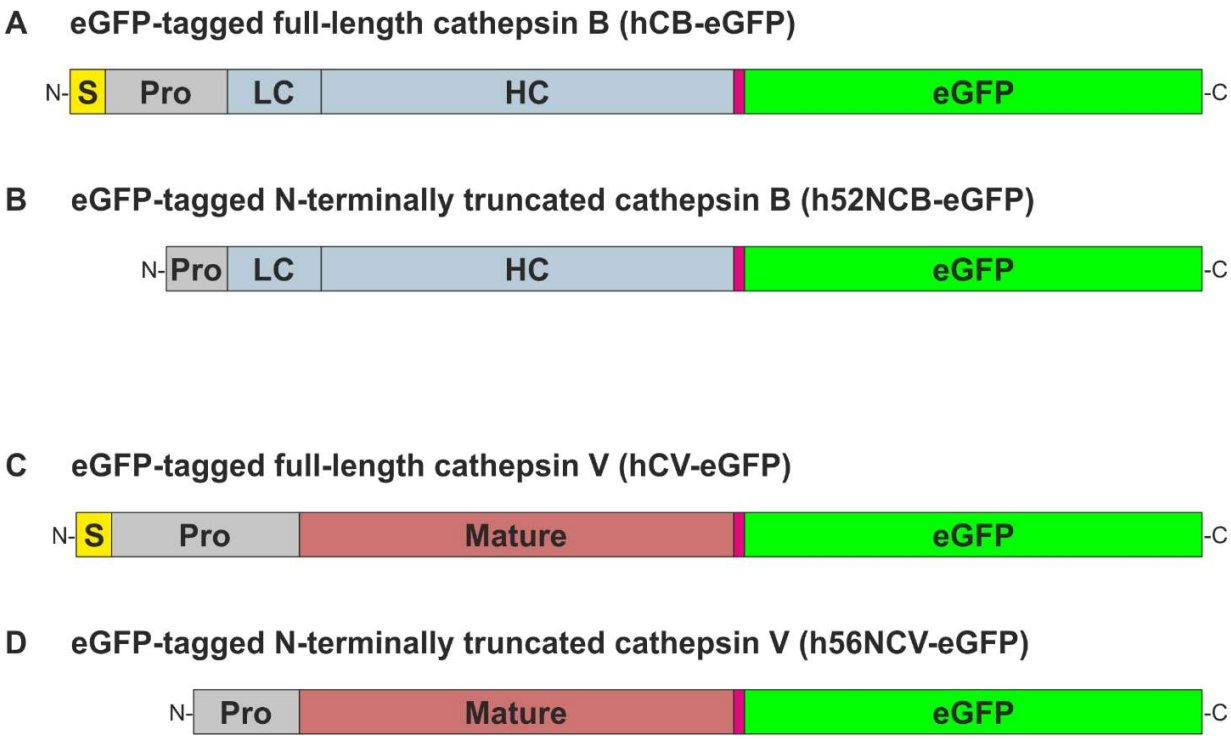

Figure 1: Schematic illustration of eGFP-tagged full-length and N-terminally truncated cathepsin chimeric proteins. **(A)** Full-length human cathepsin B (protein accession number P07858) consists of a 17-amino acid ER-targeting signal peptide (S), a 62-amino acid inhibitory propeptide (Pro), and the mature form composed of the 47-amino acid light chain (LC) and the 207-amino acid heavy chain (HC), which are held together by disulfide bonds. **(B)** The N-terminally truncated cathepsin B lacks 52 amino acids, namely, the 17-amino acid signal peptide and the initial 35-amino acid part of the propeptide. **(C)** Full-length human cathepsin V (protein accession number O60911) consists of a 17-amino acid ER-targeting signal peptide (S), a 96-amino acid inhibitory propeptide (Pro), and the 221-amino acid mature form (Mature), whereas **(D)** N-terminally truncated cathepsin V lacks the first 56 amino acids, i.e., the 17-amino acid signal peptide and the initial 39-amino acid part of the propeptide. The C-terminus of full-length and truncated cathepsins B and V, respectively, were covalently linked to eGFP (green) by a spacer peptide (pink). Letters denote the N- and C-termini, respectively.

PCR amplifications were performed using Phusion high-fidelity DNA polymerase (#M0530, NEB, Frankfurt am Main, Germany) in a Mastercycler Gradient (Eppendorf, Hamburg, Germany). The bands corresponding to cathepsin cDNA amplicons at ~1 kb were cut out of 1% agarose gels and purified using the NucleoSpin Gel and PCR Clean-Up kit (#740609 Macherey-Nagel, Düren, Germany) for subsequent insertion into the linearized pEGFP-N1 vector using T4-DNA ligase (#EL0011, Thermo Scientific, Schwerte, Germany). The ligation products were used to transform competent *E. coli* DH5α cells, and the recombinant vectors were extracted from kanamycin-resistant colonies by using the GeneJET Plasmid Miniprep Kit (#K0502, Thermo Scientific).

Following the protocol described above, the sequences coding for full-length or N-terminally truncated cathepsin V, respectively, were also inserted into puc2CL6Ipwo lentiviral vectors

upstream of the eGFP and the puromycin resistance genes [19, 20] by using *Xho*I and *Age*I restriction enzymes. Hereby, two lentiviral vectors were constructed to generate stable cell lines expressing full-length or N-terminally truncated cathepsin V protein fused at the C-terminus with eGFP. Verification of the cDNA sequences of human full-length cathepsin V fused with eGFP (hCV-eGFP) and human N-terminally truncated cathepsin V fused with eGFP (h56NCV-eGFP) in either, the *p*EGFP-N1 expression or the puc2CL6Ipwo lentiviral vectors, were confirmed by sequencing at Eurofins Genomics (Ebersberg, Germany) using forward (5'--GTCGTAACAACTCCGCCC-3') and reverse primers (5'-GTCCAGCTCGACCAGGATG-3'), or oSF031 forward (5'-CGGCGCGCCAGTCCTCCG-3') and oSF031 reverse (5'-TAGACAAACGCACACCGG-3') primers, respectively.

2.2 Cell culture

HEK 293T cells (ACC 635, *Deutsche Sammlung von Mikroorganismen und Zellkulturen* (DSMZ), Braunschweig, Germany), human thyroid epithelial cells (Nthy-ori 3-1), and the human thyroid carcinoma cell lines KTC-1 and HTh74 were grown at 37°C in a humidified atmosphere of 5% CO_2. HEK 293T cells were cultured in Dulbecco's modified Eagle's medium (DMEM; BE12-604F, Lonza, Verviers, Belgium) with 2 mM glutamine, Nthy-ori 3-1 and KTC-1 in Roswell Park Memorial Institute medium (RPMI 1640, 12-702F, Lonza), and HTh74 in Eagle´s Minimum Essential Medium (EMEM, BE06-174G, Lonza), all supplemented with 10% fetal calf serum (origin Brazil, Thermo Fisher Scientific, Darmstadt, Germany).

2.3 Generation of stable cell lines

Transduction of the Nthy-ori 3-1 cell line was performed as described previously [19-21]. To prepare lentiviral particles, the packaging HEK293T cells were grown to 70% confluence and co-transfected with three different plasmids, i.e. the transfer plasmid carrying the gene of interest, namely, puc2CL6Ipwo-hCV-eGFP or puc2CL6Ipwo-h56NCV-eGFP, respectively, the envelope plasmid carrying the gene for the vesicular stomatitis virus glycoprotein (VSV-G), and the helper plasmid (pCDNL-BH). Integration of the gene of interest into the host cells is achieved by infecting them with lentiviral particles containing reverse transcriptase and integrase to retrotranscribe the RNA into DNA for subsequent integration into the host genome, respectively. Transfection was performed using 45 µL of polyethylenimine (PEI) (1 mg/mL; #40872, Sigma Aldrich, Taufkirchen, Germany) and 6 µg of each plasmid. Two days post transfection, medium containing lentiviral particles was collected from the packaging HEK293T cells, and viral particles were collected upon filtration through 0.45 µM porous membranes (# 16555K, OMNILAB, Bremen, Germany). The viral supernatants were stored for up to 7 days at 4°C.

To transduce target cells like the Nthy-ori 3-1 cells, they were seeded in complete culture medium in 6-well plates. When cells reached 30% confluence, they were incubated with viral supernatants for 24 h in complete culture medium. Afterwards, the transduced cells were selected in medium supplemented with 1 µg/ml puromycin (#0240, Carl Roth GmbH, Karlsruhe, Germany) for 6 days. To this end, we have established two cell lines stably expressing full-length and N-terminally truncated cathepsin V, which are henceforth referred to as Nthyori-CV and Nthyori-NCV, respectively.

2.4 Transient transfection

Nthy-ori 3-1 cells were transiently transfected with *p*CB-eGFP, *p*h52NCB-eGFP, *p*CV-eGFP, or *p*h56NCV-eGFP, respectively, by X-treme GENE HP DNA transfection reagent (#6366244001, Roche Diagnostics, Mannheim, Germany) as described in the manufacturer's protocol. In brief, the conditions to reach optimal transfection efficiencies of cells grown in 6-well plates were typically achieved using 2 µg plasmid DNA and 6 µl transfection reagent per well.

2.5 Cell synchronization

In order to synchronize cells in G_0/G_1 phase, confluent cultures were incubated in serum free-medium for 48 h. Cells were arrested in S phase by a double-thymidine block, i.e. cells were grown to 30-40% confluence in complete culture medium before incubation in complete culture medium supplemented with 2 mM thymidine (# 3005.1, Carl Roth GmbH) for 18 h. After the first thymidine block, cells were incubated in complete culture medium for 9 h, and treated with 2 mM thymidine for another 17 h. For synchronization in M phase, cells at 30-40% confluence were first treated with 2 mM thymidine for 18 h, which was followed by incubation in complete culture medium for 3 h. Afterwards, cells were incubated with 100 ng/ml nocodazole (#M1404, Sigma Aldrich) for 12 h. Synchronized cells were either fixed and processed for immunofluorescence, or collected and prepared for flow cytometry analyses.

2.6 Flow cytometry analysis

In order to determine expression of eGFP-tagged protein throughout the cell cycle, synchronized cells were trypsinized and collected by centrifugation for 5 min at 200 xg. Following washing twice with PBS and resuspending the cells in 1 ml PBS, the fluorescence intensity of eGFP was determined using a CyFlow Space flow cytometer (Sysmex, Dresden, Germany). Data was analyzed using FlowJo software (Tree Star, Ashland, USA). Results are given as means ± standard deviations (SD) of three independent experiments.

2.7 Cell proliferation assay

Cell proliferation rates and metabolic activity levels of cells were evaluated by an assay that is based on the ability of dehydrogenases of metabolically active cells to reduce yellow MTT reagent (3(4,5-dimethylthiazol-2-yl)-2,5-diphenyltetrazolium bromide; Carl Roth GmbH) to water-insoluble violet-blue formazan, the MTT assay. The amount of formazan, which is directly proportional to the culture's metabolic activity, i.e. thereby determining cell viability and proliferation rates, is quantified by spectrophotometry. Cells were seeded in 24-well plates at a density of 5 x 10^4 cells/well. After 24 h, cells were incubated with fresh complete culture medium containing MTT at a final concentration of 0.5 mg/ml for 2 h. Then, the supernatant was discarded and 1 ml DMSO was added to each well to dissolve formazan, which was quantified at 595 nm with a spectrophotometer. Results are presented as mean values and standard deviations (SD) from three independent experiments, each consisting of three technical replicates.

2.8 Cell proliferation rate determination by growth curves

Cell proliferation rates were also determined by growth curves upon seeding cells into 6-well plates at a density of 4 × 10^4 cells/well and their enumeration after different time intervals, i.e., 16, 24, 48, and 72 h. Trypsin-dislodged cells were counted using a Neubauer hemocytometer. The results are given as the averages of two independent experiments with three replicates each.

2.9 Indirect immunofluorescence

Cells were immunolabeled as described before [22]. Briefly, cells fixed with 4% paraformaldehyde were permeabilized by incubation in 0.2% Triton X-100 in CMF-PBS for 5 min. After blocking with 3% bovine serum albumin in CMF-PBS for 1 h at 37 °C, cells were incubated with primary antibodies diluted in 0.1% BSA in CMF-PBS overnight at 4°C. In this study, the following primary antibodies were used, namely, goat anti-mouse cathepsin B (1:100; #GT15047, Neuromics, Hiddenhausen, Germany), monoclonal mouse anti-human procathepsin V clone CV55-1C5 (1:100; produced by EW), mouse anti-human cathepsin V (1:50; #MAB1080, R&D Systems, Minneapolis, USA), and rabbit anti-Ki67 (1:100; #16667, Abcam, Cambridge, UK). Secondary antibodies conjugated with Alexa 488 or Alexa 546 (1:200; Molecular Probes, Karlsruhe, Germany) were diluted in 0.1% BSA in CMF-PBS and incubated for 60 minutes at 37°C. DRAQ5™ (Biostatus Limited, Shepshed Leicestershire, UK) was added at a final concentration of 5 µM to the secondary antibody mixtures to counter-stain nuclear DNA.

Immunohistochemistry was performed on paraffin-embedded human thyroid tissue sections. Human thyroid tissue was obtained from patients undergoing thyroid surgery and used in compliance with the Helsinki Declaration. The tissue was fixed in paraformaldehyde, embedded

in paraffin and sectioned as described [23]. Then, the sections were deparaffinized by immersing them in xylol 4 times for 5 min each, and rehydrated by dipping them sequentially in a graded series of ethanol, i.e., 100, 95, 70, and 30% of ethanol (V/V) was used for 5 min each. Autofluorescence was reduced by incubating the sections in freshly prepared sodium borohydride (1% in water; Carl Roth GmbH) for 5 min at room temperature. Subsequently, blocking and antibody incubations were performed as described above.

2.10 Image acquisition and analysis

Thyroid tissue sections and stably or transiently expressing or non-transduced cells were imaged upon staining using a confocal laser scanning microscope (LSM 510 Meta, Carl Zeiss Jena GmbH, Jena, Germany). Micrographs were obtained at a pinhole setting of one Airy unit at resolutions of 1024 × 1024 pixels, and analyzed with standard LSM 510 or Zen 2012 software (Carl Zeiss Jena GmbH). To determine the ratio of nuclear to cellular cathepsins for each cell, intensities of immunostaining or eGFP signals over the areas covered by the nuclei, which were identified by masking the corresponding Draq5-positive area, as well as total signal intensities were quantified by using open source software Cell Profiler [24]. The pipeline consisted of sequential sets of automated image analysis modules (Fig. 2). The first module 'Color To Gray' splits the loaded original image into two channels, namely red and green channels, and then converts them into grayscale, resulting in two separate images called OrigRed, and OrigGreen corresponding to Draq5 and immunostaining or eGFP signals, respectively. The second module 'IdentifyPrimaryObjects' aims to identify the nuclei from the OrigRed image based on the typical diameter ranging from 15 to 140 pixels, i.e. these values need to be adjusted to the respective image resolution. To identify the cells from the OrigGreen image, the third module 'IdentifySecondaryObjects' used the nuclei as seeds to detect the cell outlines, using watershed-imaging methods. Next, the 'IdentifyTertiaryObjects' module identified the cytoplasm by subtracting the area covered by nuclei from the total cell area. The cells touching the borders of the image were removed by using the option 'Image or mask border' in a module called 'FilterObjects'. Once the filtered objects were identified, the intensities of green signals over the area of cells, cytoplasm and nuclei were measured using the 'MeasureObjectIntensites' module. It is important to note that a threshold for cathepsin-positivity was set such that more than 50% of the nuclear profiles needed to be covered with cathepsin-specific signal to be counted as a positive event (see Fig. 3). The number of Ki67-positive cells over all cells was also determined by Cell Profiler using the steps described [25] to quantify proliferation rates.

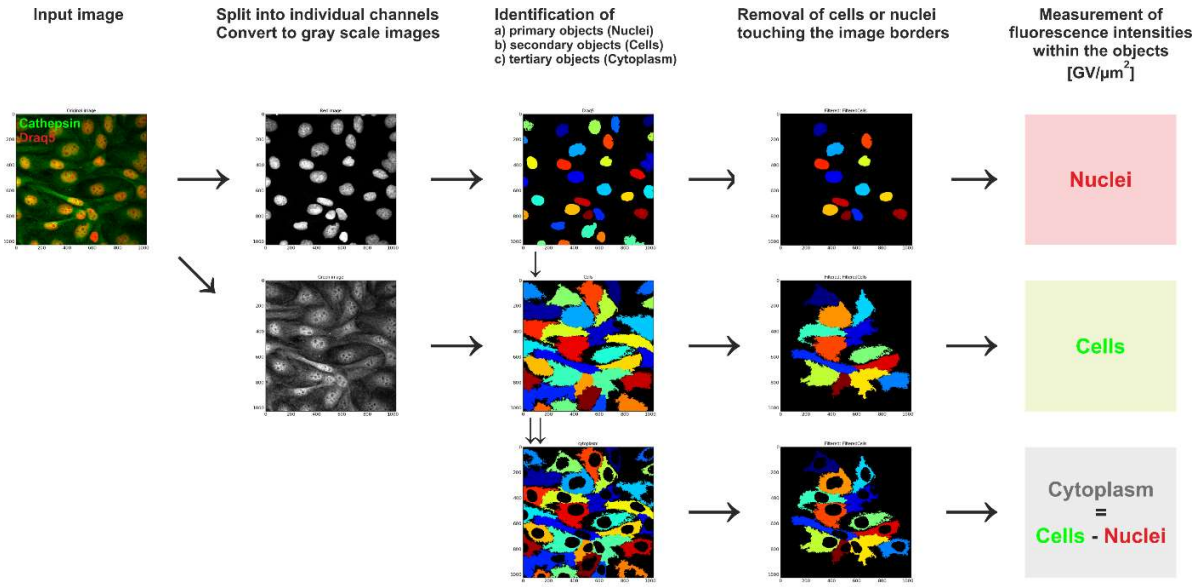

Figure 2: Automated image analysis pipeline for quantifying expression of cathepsins in thyrocytes. Schematic diagram depicting the Cell Profiler modules used for quantification of the proportion of nuclear cathepsins in human thyroid epithelial cells immunostained with cathepsin-specific antibodies or transduced with eGFP-tagged full-length and N-terminally truncated cathepsins. **(i)** The input image is a two-channel merged picture representing immunostaining or eGFP fluorescence (green signals) and Draq5-stained nuclear DNA (red signals). **(ii)** The input image was split into two individual channels, namely, OrigRed and OrigGreen, and converted to gray scale. **(iii)** The OrigRed image was used to identify the nuclei. These were used as seeds to identify individual cells through propagation toward the cell surface. Subtracting the area covered by nuclei from the respective cellular area yielded the cytoplasm area. **(iv)** Objects touching the borders of an image were taken out of further analyses. **(v)** The intensities of fluorescence signals within cellular, cytoplasmic, and nuclear areas were quantified, respectively. Finally, percentages of nuclear *versus* total cellular fluorescence signals were calculated as given in individual figure captions.

2.11 Cell lysate preparation, SDS-PAGE and immunoblotting

After washing twice with ice-cold PBS, cells were harvested by using a cell scraper and collected by centrifugation for 5 min at 200 xg at 4°C. The cell pellets were resuspended in lysis buffer consisting of 0.2% Triton X-100 in PBS, pH 7.4, supplemented with protease inhibitors, i.e. 10 µM E64, 1 µM Pepstatin A, 2 ng/ml Aprotinin, 0.02 M EDTA, and incubated for 30 min at 4°C on an end-over-end rotator. The supernatants were cleared by centrifugation for 10 min at 16,000 *g* at 4 °C, and stored at −20 °C. The Neuhoff assay [26] was used to determine protein concentrations. The samples were normalized to equal amounts of protein and mixed with sample buffer consisting of 50 mM Tris-HCl (pH 7.6), 2.5% sodium dodecyl sulphate (SDS), 125 mM dithiotreitol (DTT), 50% glycerol, and 4 µM bromophenol blue. After heating the samples for 5 min, they were loaded along with a PageRuler Prestained Protein ladder (#P7712S, NEB) and separated on 12.5% SDS-gels, before proteins were transferred onto nitrocellulose membranes by semi-dry blotting for 45 min at 25 V. To prevent non-specific binding of primary and secondary antibodies, membranes were incubated with 5% milk powder in PBS-T, consisting of 11.7 mM NaH_2PO_4, 63.2 mM Na_2HPO_4, 68 mM NaCl, pH 7.2, supplemented with 0.3% Tween-20 overnight at 4°C. Membranes were then incubated with primary antibodies, i.e., mouse anti-GFP (#1814460,

Roche) diluted in 2.5% milk powder in PBS-T for 1 h at room temperature. After washing 6 times for 5 min each in PBS-T, blots were incubated with horseradish peroxidase (HRP)-conjugated IgG secondary antibodies, namely goat anti-mouse (Southern Biotech, Birmingham, USA) for 1 h at room temperature. Blots were washed again and incubated with chemiluminescent substrate (#34580, Thermo Scientific) for 3 min at room temperature before visualization through enhanced chemiluminescence on XPosure™ films (Thermo Scientific).

2.12 Statistical analysis

Data was analyzed by the use of GraphPad Prism 5.01 software (GraphPad, San Diego, California, USA). Levels of statistical significance were determined by one-way ANOVA, followed by Tukey *post hoc* tests. Values of $p < 0.05$ were considered statistically significant.

3. Results

3.1 Nuclear Cathepsin V in Thyroid Tissue

Localization of cathepsins B and V was examined in human thyroid tissue sections obtained from different conditions, i.e. hot nodules, cold nodules, goiter, papillary thyroid carcinoma (PTC), and follicular thyroid carcinoma (FTC) tissue was used for immunostaining (Fig. 3, A1-E1). As expected, cathepsin B was found within vesicles scattered throughout the cytoplasm in all tissues examined (Fig. 3, A2-E2). In addition, and as expected from our previous studies [11], cathepsin B-positive vesicles were abundantly detected at the basolateral pole of thyroid cells in PTC (Fig. 3, D2). Cathepsin V-immunopositive signals were likewise observed in a vesicular pattern in the cytoplasm of thyroid tissue cells (Fig. 3, A3-E3). However, cathepsin V was additionally and mainly detectable in the nuclei of thyroid tissue cells, most prominently in biopsies from cold nodules and in FTC or PTC (Fig. 3, B3, D3, E3, respectively). Interestingly, nuclear cathepsin V was much less abundant in hyper-functional hot nodule thyroid tissue (Fig. 3, A3), and in the nuclei of few cells in goiter tissue (Fig. 3, C3), which both are not considered cancer tissue.

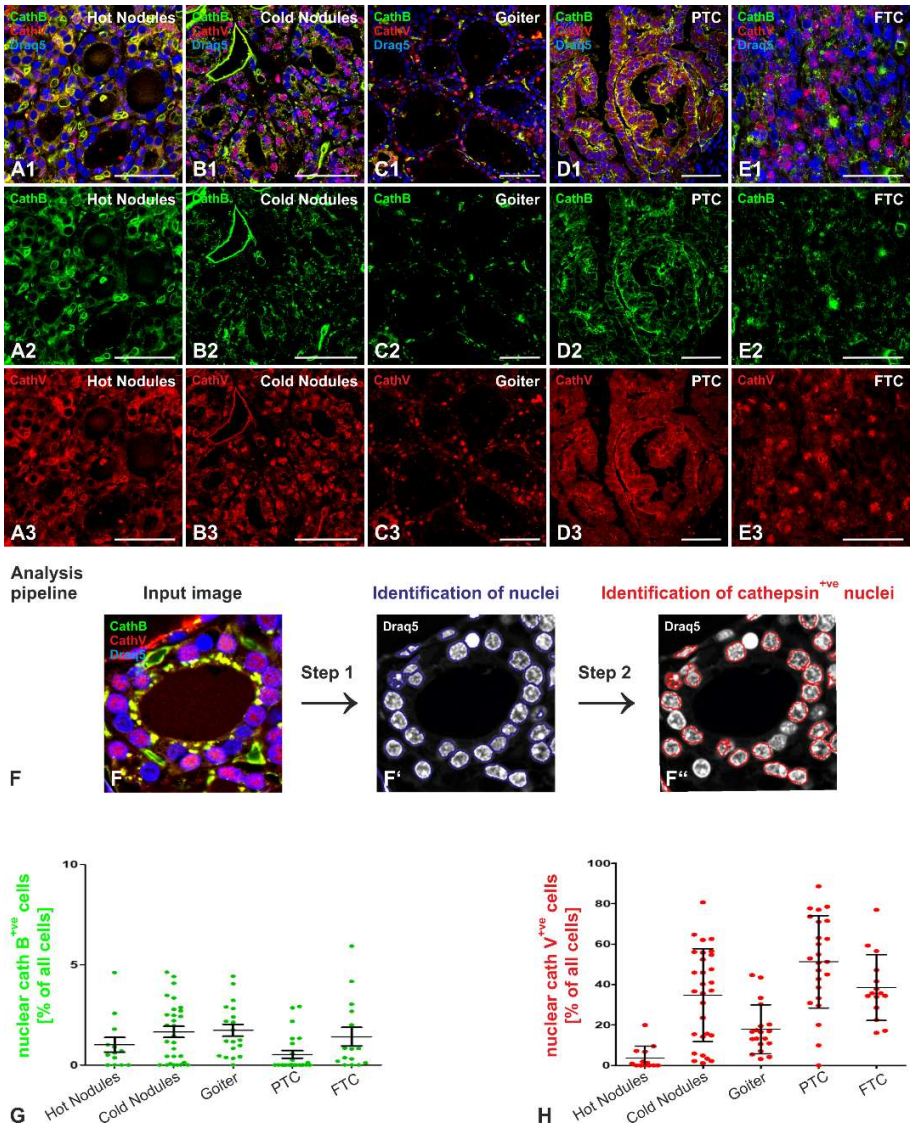

Figure 3: Immunohistochemistry of cysteine cathepsins in thyroid tissue. Human thyroid tissue sections from different pathological conditions, i.e. hot nodules (A1-A3), cold nodules (B1-B3), goiter (C1-C3), PTC (D1-D3), and FTC (E1-E3), were immunolabeled with cathepsin B- (green signals in A1-E1 and A2-E2) and cathepsin V-specific antibodies (red signals in A1-E1 and A3-E3). Nuclei were counter-stained with Draq5™ (blue signals in A1-E1). The images were taken with a confocal laser scanning microscope. Corresponding single channel and merged fluorescence micrographs are depicted as indicated. A Cell Profiler pipeline (F) was set up to identify the Draq5™–positive nuclear profiles (F'). The numbers of nuclear profiles containing cathepsins B or V covering more than 50% of their areas were determined (F''), and are depicted as percentages of all cells with Draq5-positive nuclear areas (G and H). The results showed that nuclear profiles of less than 5% of the cells were cathepsin B-positive (G), whereas cathepsin V-specific staining was observed in many nuclei (H). Note that higher numbers of cathepsin V-containing nuclei were detected in cold nodules and in thyroid carcinoma tissue in comparison with hot nodules and goiter tissue (H). Data are presented as scatter graphs in which the means ± SD are indicated (G and H). The numbers of individual cells analyzed were n= 4350 for hot nodules, n= 10368 for cold nodules, n= 5010 for goiter, n= 7358 for PTC, and n=4790 for FTC tissue, respectively.

Cold nodules are considered non-functional thyroid tissue bearing higher risk of developing into malignant cancers than hot nodules that preserve thyroid functional features. Hence, we thought to quantify the number of cells with nuclear cathepsin V immunosignals in the different thyroid tissue samples (Fig. 3, F). Quantification of fluorescence signal intensities over nuclear profiles revealed that nuclei were only occasionally anti-cathepsin B-positive (Fig. 3, G), whereas cathepsin V-specific staining was observed in the cellular nuclei of all tissues analyzed (Fig. 3, H). Note that significantly higher numbers of cathepsin V-containing nuclei were detected in the cells of cold nodule and thyroid carcinoma tissue, i.e. PTC and FTC, in comparison with hot nodules and goiter tissues (Fig. 3, H). These findings pointed to a potential role of nuclear cathepsin V as a biomarker of thyroid cancer, and prompted us to investigate the localization and expression of cathepsin V in human thyroid epithelial cells in greater detail with the aim to establish a cellular model for mechanistic studies.

3.2 Characterization of epithelial and mesenchymal features of thyroid cell lines

In this study, human thyroid epithelial cells (Nthy-ori 3-1) and two different thyroid carcinoma cell lines, namely, KTC-1 and HTh74 derived from poorly differentiated papillary and anaplastic thyroid carcinoma, respectively, were used to represent different stages of epithelial-to-mesenchymal transition (EMT) observed in normal thyroid tissue and thyroid carcinoma. E-cadherin, claudin-1, and occludin were used as epithelial markers, while vimentin was used as a mesenchymal marker in immunofluorescence staining experiments. Proteins typically expressed by epithelial cells were detectable in all cell lines when grown in high-density to confluent cultures (Fig. 4). In particular, the PTC-representative KTC-1 cells exhibited epithelial features as they maintain cell-to-cell adherens junctions (AJ) and tight junctions (TJ) as obvious from the E-cadherin, claudin-1 and occludin-positive staining patterns along the lateral cell borders (Fig. 4, B1-3, arrowheads). However, Nthy-ori 3-1 and HTh74 displayed rather diffuse punctate signals in the cytoplasm upon immunostaining of E-cadherin, claudin-1 and occludin (Fig. 4, A1-3 and C1-3, respectively). Regarding vimentin, no staining was observed in KTC-1 cells (Fig. 4, B4), whereas this mesenchymal marker was abundant in the cytosol of Nthy-ori 3-1 and HTh74 cells (Fig. 4, A4 and C4, respectively). HTh74 cells exhibited vimentin-build filamentous structures throughout the cytoplasm (Fig. 4, C4, arrows), while these were less abundant in Nthy-ori 3-1 cells (Fig. 4, A4, arrows).

The data indicated that the cell lines used in this study represent distinct stages in EMT as an important precondition to our proposal of using them as cellular models representing thyroid epithelial or carcinoma cells. KTC-1 exhibited the most epithelial-like features, although originally derived from PTC tissue, while Nthy-ori 3-1 and HTh74 cells acquired mesenchymal

characteristics to different extents. Not astonishingly, HTh74 cells were the most dedifferentiated in comparison to the other cell lines as expected from their ATC origin. Next, we used these cell lines to check whether the localization of the cathepsins B and V correlated with their respective EMT states.

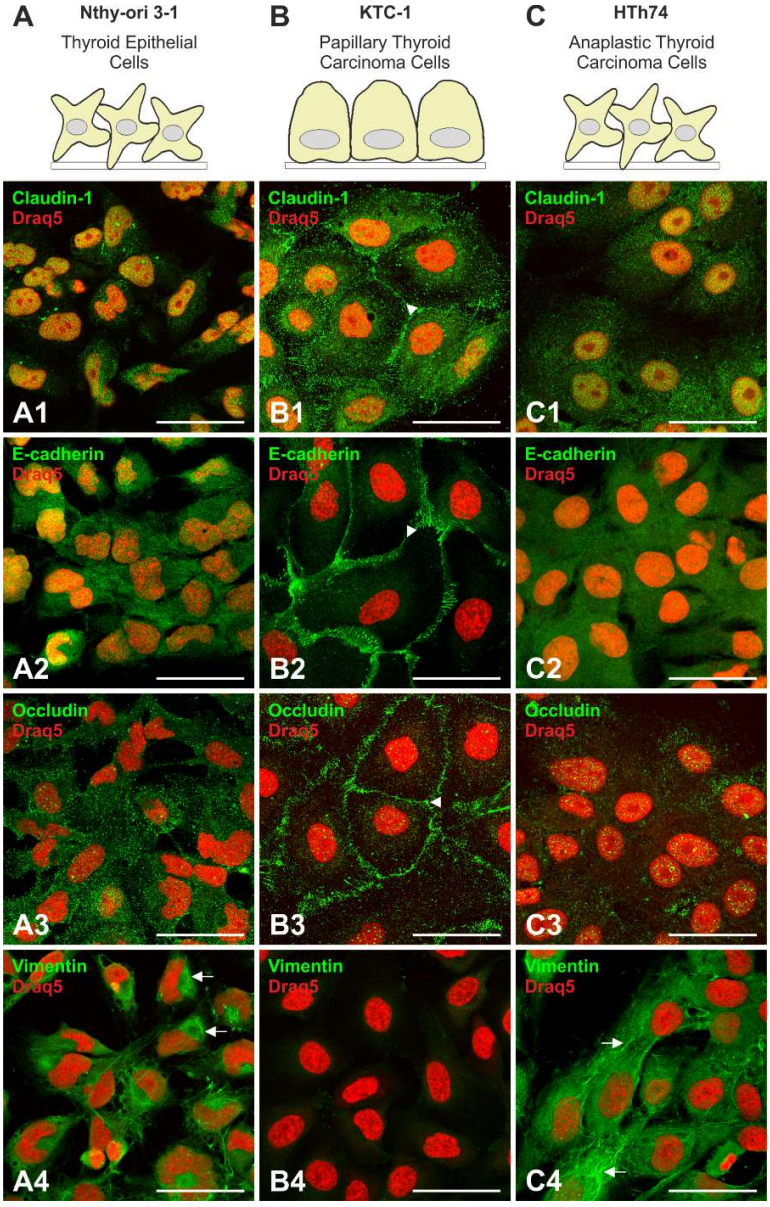

Figure 4: Epithelial and mesenchymal characteristics of Nthy-ori 3-1, KTC-1, and HTh74 cells. Nthy-ori 3-1 (A-A4), KTC-1 (B-B4), and HTh74 (C-C4) cells are schematically depicted (A-C). They were immunolabeled with antibodies against epithelial and mesenchymal markers (green signals), namely, claudin-1 (A1-C1), E-cadherin (A2-C2), occludin (A3-C3), and vimentin (A4-C4), respectively. Nuclei were counter-stained with Draq5 (red signals in A1-C4). KTC-1 cells, only, displayed the expected staining at lateral borders between neighboring cells (arrowheads), indicating typical epithelial cell-cell contacts *via* AJ (B2) and TJ (B1, B3) proteins. However, Nthy-ori 3-1 (A1-A3) and HTh74 cells (C1-C3) revealed non-epithelial cytosolic localization patterns of junctional proteins. The mesenchymal marker vimentin was detected in filament-like structures (arrows) in Nthy-ori 3-1 (A4) and HTh74 cells (C4), while no obvious vimentin staining was observed in KTC-1 cells (B4). Scale bars represent 50 µm.

3.3 Cathepsin V is the predominant cysteine cathepsin in the nuclei of thyroid cell lines in steady state

To determine the subcellular localization of cathepsins B and V in the cell lines Nthy-ori 3-1, KTC-1 and HTh74 in steady state, the cells were immunolabeled in sub-confluent to near-confluent cultures. Cathepsin B immunostaining highlighted predominately vesicles accumulating in the perinuclear region of the cells in steady state, i.e. the endo-lysosomes (Fig. 5, A1-A3, arrows). In addition, the nuclei of Nthy-ori 3-1, KTC-1 and HTh74 cells were also immunostained to some extent (Fig. 5, A1-A3, bottom right panels), which was reported previously by our group [8]. In clear contrast, a pronounced nuclear localization of cathepsin V was observed throughout the nuclear matrix, while excluding the nucleoli of all immunolabeled cell lines (Fig. 5, B1-B3). Furthermore, a much weaker cytoplasmic signal for anti-cathepsin V-positive structures was observed in all three cell lines, i.e. Nthy-ori 3-1, KTC-1 and HTh74 cells (Fig. 5, B1-B3), but this was not reticular or vesicular as observed for cathepsin B. The data pointed to predominantly canonical sorting and transport of cathepsin B along the secretory pathway, whereas cathepsin V forms reached the nuclear compartment of the thyroid cell lines investigated in this study.

The proportions of nuclear versus total cathepsin B and V-positive immunosignals were determined by quantifying the ratios of nuclear over total cellular fluorescence signal intensities of immunolabelled cells (Fig. 5, C). Quantification analysis showed that cathepsin V-immunopositive fluorescence was significantly more prominently present in the nuclei of all three cell lines than that of cathepsin B, demonstrating a nuclear to cellular ratio of cathepsin V immunofluorescence ranging from 25% to 50% in each and all of the three cell lines (Fig. 5, C, dark grey bars). Therefore, we focused our further experiments on cathepsin V.

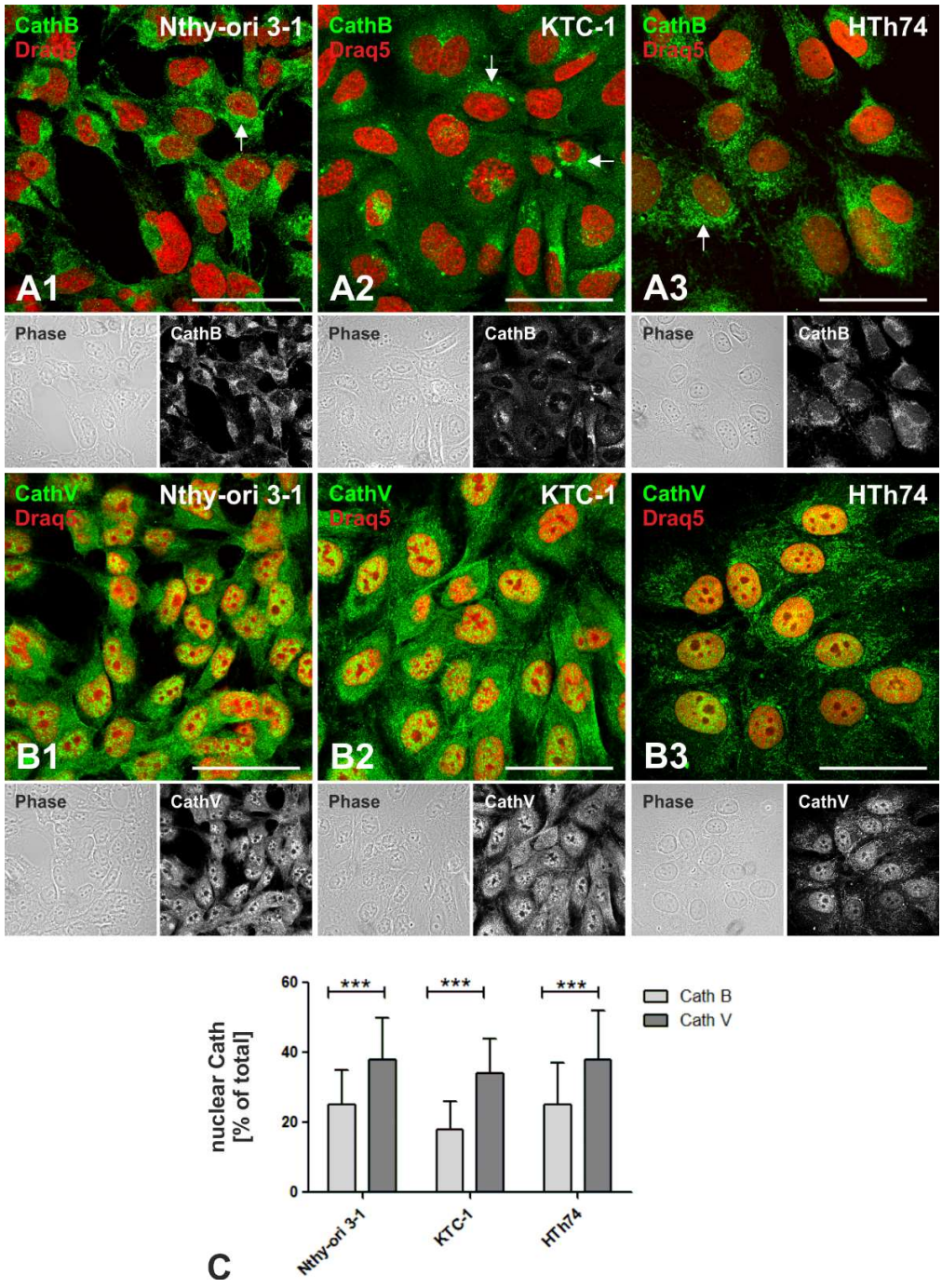

Figure 5: Localization of cathepsins B and V in thyroid epithelial and carcinoma cell lines. Nthy-ori 3-1, KTC-1, and HTh74 cells were immunolabeled with cathepsin B- (A1-A3) and V- (B1-B3) specific antibodies (green signals). Nuclei were counter-stained with Draq5 (red signals). Single-channel fluorescence and corresponding phase contrast micrographs are depicted in bottom panels as indicated. Cathepsin B was mainly observed in vesicles scattered throughout the cytosol and accumulating in the perinuclear regions of all three cell lines analyzed (A1-A3, arrows), while cathepsin V was localized in the nucleoplasm excluding the nucleoli (B1-B3). Scale bars represent 50 µm. The bar chart in C represents the percentages of nuclear over total cellular fluorescence intensities of cathepsin B (light grey) and cathepsin V (dark grey), respectively, in Nthy-ori 3-1, KTC-1, and HTh74 cells as indicated. Cathepsin immunopositive signals were quantified by analyzing at least 400 cells per each cell line through a Cell Profiler pipeline. Data are depicted as means + SD. Levels of significance were determined by two-tailed, unpaired Student's t-test and are indicated as *** for $p < 0.001$.

3.4 Sub-nuclear cathepsin V localization throughout the cell cycle of thyroid epithelial and carcinoma cells

Because cathepsin V was present in the nuclei of thyroid cells with epithelial features and more abundantly in dedifferentiated cells featuring mesenchymal markers, we were interested to investigate whether the localization and/or the amounts of cathepsin V in the nucleus might change in different phases of the cell cycle.

A growing cell culture is normally composed of cells that progress through any and all stages of the cell cycle (Fig. 6, A1). Nthy-ori 3-1, KTC-1, and HTh74 cell cultures were synchronized and the cells were arrested in different cell cycle phases (Fig. 6, A2-A4), i.e. in G_0/G_1 by growth factors deprivation, in S phase by a double-thymidine block, and in G_2/M phase by treatment with nocodazole. To verify that the cells were arrested in the desired phases, they were immunolabeled with antibodies against the proliferation marker Ki67 (Fig. 6, A1-A4). Ki67 is expressed throughout the cell cycle except in G_0 phase [27, 28]. During G_1 phase, Ki67 was observed in small discrete foci throughout the nucleoplasm of few cells (Fig. 6, A2), whereas it was detected in a limited number of larger foci during S phase (Fig.6, A3). Cells synchronized in G_2/M phase displayed an intense staining of Ki67 associated with condensed chromatin (Fig.6, A4). The results of Ki67 immunostaining verified that the three cell lines, i.e. Nthy-ori 3-1 (Fig. 6, B1-D1), KTC-1 (Fig. 6, B2-D2), and HTh74 cells (Fig. 6, B3-D3), were successfully arrested at G_0/G_1, S, and G_2/M phase, respectively. Interestingly, cells of all three lines displayed nuclear localization of cathepsin V throughout each and all phases of the cell cycle (Fig. 6, B1-D3), but the most prominent nuclear cathepsin V immunostaining signals were observed in S-phase arrested cells (Fig. 6, C1-C3). Quantification of the ratios of nuclear versus total cathepsin V immunopositive signals, as determined semi-automatically using a Cell Profiler pipeline, demonstrated that the ratio of nuclear over total cellular cathepsin V was highest in S phase, and significantly exceeded its nuclear presence in the G_0/G_1 and G_2/M phase-arrested cells of all three cell lines examined (Fig. 6, E1-E3, respectively). These data support the hypothesis that the amounts of nuclear cathepsin V peak in S phase. Thus, nuclear cathepsin V could possibly be involved in regulation of cell cycle progression particularly in S-phase, i.e. shortly before the cells start to divide mitotically.

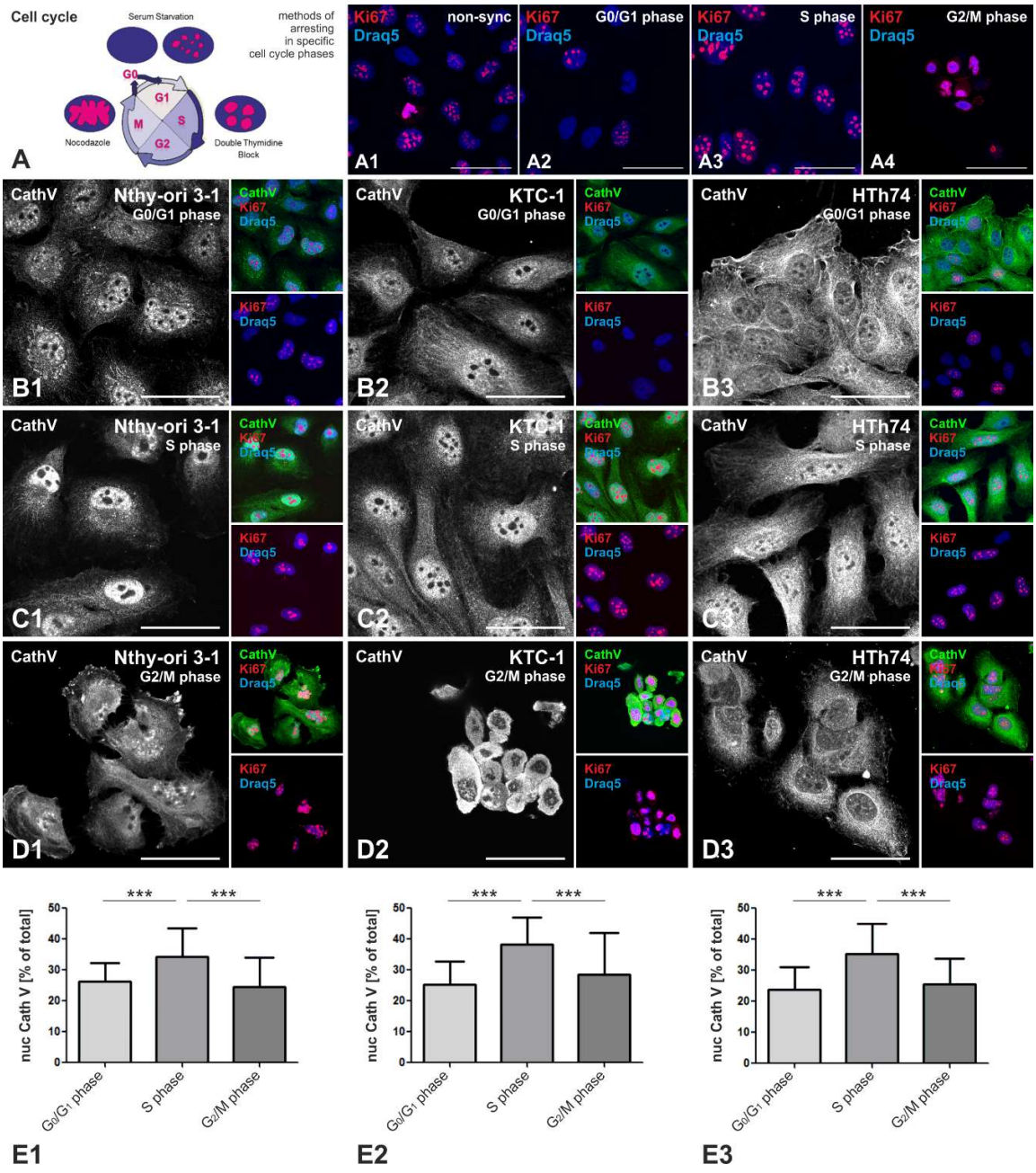

Figure 6: Localization of cathepsin V throughout the cell cycle of thyroid epithelial and carcinoma cells. Sketch depicting schematically the intranuclear distribution of Ki67 throughout the cell cycle is shown and the methods used to arrest cells in specific cell cycle phases are illustrated (A). Fluorescence micrographs of cells immunolabeled with Ki67-specific antibodies (red) and upon counter-staining of nuclear DNA with Draq5 (blue) after synchronization in distinct cell cycle stages revealed the typical sub-nuclear patterns of the Ki67 proliferation marker (A1-A4, pink as a result of overlapping red and blue signals). Nthy-ori 3-1, KTC-1, and HTh74 cells were synchronized in different cell cycle phases, i.e. G_0/G_1 (B1-B3), S (C1-C3), and G_2/M phase (D1-D3). The synchronized cells were immunolabeled with antibodies against cathepsin V (grey and green signals) and Ki67 (red signals), while nuclei were counter-stained with Draq5 (blue signals). Corresponding single channel and merged fluorescence micrographs are displayed as indicated. Scale bars represent 50 µm. The percentages of nuclear over cellular cathepsin V immuno-positive signals at different cell cycle stages are depicted in bar charts for Nthy-ori 3-1 (E1), KTC-1 (E2), and HTh74 cells (E3). Quantification was performed with at least 200 cells for each cell cycle phase and cell line, respectively. Data are depicted as means + SD. Levels of significance were determined by one-way ANOVA followed by Tukey *post hoc* test and are indicated as *** for $p < 0.001$.

3.5 Pro-cathepsin V is not localized to the nuclei of thyroid epithelial and carcinoma cells *in vitro*

We have previously reported that cathepsin L reaches the nuclei of colorectal carcinoma cells [25], while a specific 40 kDa-form of cathepsin B reaches the nuclei of ATC cells [8]. Thus, sorting and trafficking of distinct cysteine cathepsins seems to differ among epithelial and carcinoma cell types, and might depend upon the enzyme itself. Hence, we asked next whether cathepsin V reaches the nucleus of the thyroid epithelial and carcinoma cell lines investigated in this study as full-length and endo-lysosomally matured form due to leaky compartments, or alternatively, is destined to the nucleus upon cytosolic translation of a specific form.

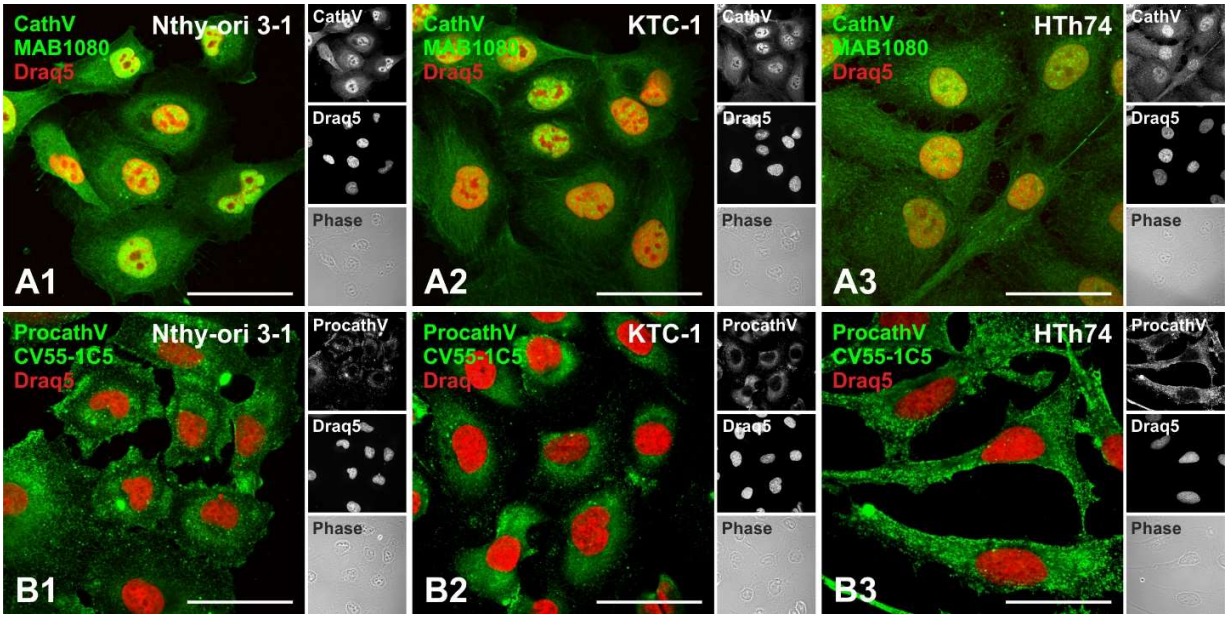

Figure 7: Procathepsin V is not present in the nuclei of thyroid epithelial and carcinoma cells. Confocal laser scanning micrographs of Nthy-ori 3-1, KTC-1, and HTh74 cells immunolabeled with different cathepsin V antibodies (green signals), namely, anti-human cathepsin V MAB1080 (A1-A3) recognizing both the pro- and mature cathepsin V forms, and anti-human cathepsin V CV55-1C5 (B1-B3) that exclusively immunoreacts with the proform of cathepsin V. Nuclei were counter-stained with Draq5 (red signals). Single channel fluorescence and corresponding phase contrast micrographs are depicted in the right panels as indicated. Scale bars represent 50 µm.

Hence, Nthy-ori 3-1, KTC-1 and HTh74 cells were immunostained with cathepsin V antibodies that detect, in principle, different forms of cathepsin V. Namely, anti-human cathepsin V MAB1080 was used, which reacts with both the pro- and mature forms, and its staining pattern was compared to that of anti-human cathepsin V CV55-1C5 that exclusively immunoreacts with the proform. Both antibodies revealed vesicular and reticular staining patterns within the cytoplasm of all three cell lines (Fig. 7). However, only cells immunolabeled with cathepsin V MAB1080 antibodies exhibited positive signals within the nuclei in addition (Fig. 7, A1-A3), while antibodies against procathepsin V (CV55-1C5) did not immunostain the nuclei of Nthy-ori 3-1, KTC-1, and HTh74 cells (Fig. 7, B1-

B3). These results indicated that the proform of cathepsin V is indeed translated into the lumen of the endoplasmic reticulum and transported along the secretory route to endo-lysosomes of Nthy-ori 3-1, KTC-1, and HTh74 cells, as expected. Importantly, procathepsin V is however not able to reach the nucleus of any of the herein investigated thyroid epithelial and carcinoma cell lines.

3.6 Localization of full-length and N-terminally truncated cathepsin B and V forms expressed as GFP-chimeras in thyroid epithelial cells

Since procathepsin V is not present in the nuclei of thyroid epithelial and carcinoma cell lines (see Fig. 7), we proposed a specific N-terminally truncated form of cathepsin V lacking the signal peptide and part of the propeptide that reaches the nucleus upon translation at cytosolic ribosomes. To test this proposal, Nthy-ori 3-1 cells were transiently transfected with plasmids coding for full-length (hCV-eGFP) and N-terminally truncated cathepsin V (h56NCV-GFP), both fused with eGFP at their C-terminus serving as an easily detectable tag (Fig. 8, see also Fig. 1). As a control, cells were transfected with vectors coding for eGFP-chimeras with full-length (hCB-eGFP) and N-terminally truncated cathepsin B (h52NCB-GFP) (Fig. 8, see also Fig. 1).

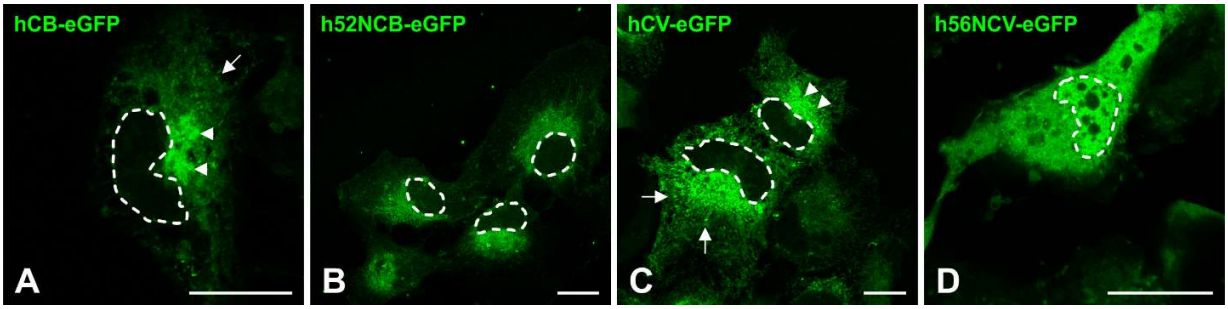

Figure 8: Localization of eGFP-tagged full-length and N-terminally truncated cathepsin B and V chimeras in thyroid epithelial cells. Single channel fluorescence micrographs (A-D) of Nthy-ori 3-1 cells after transfection with plasmids coding for eGFP-tagged full-length cathepsin B (hCB-eGFP) (A), N-terminally truncated cathepsin B (h52NCB-eGFP) (B), full-length cathepsin V (hCV-eGFP) (C), and N-terminally truncated cathepsin V (h56NCV-eGFP) (D). Nthy-ori 3-1 cells, which express hCB-eGFP and hCV-eGFP chimeras (A and C, respectively), exhibited green fluorescence within a reticular network, the Golgi apparatus (arrowheads) and vesicles (arrows). While the chimeric protein h52NCB-eGFP revealed a similar localization (B, cf. A), the chimeric protein h56NCV-eGFP was localized to the cytosol and nuclei of Nthy-ori 3-1 cells (D*).* Dotted lines represent the outlines of the respective nuclei. Scale bars represent 20 µm.

The results showed that both full-length cathepsins B and V are targeted to endo-lysosomes as expected from the canonical trafficking pathway of cysteine cathepsins bearing a signal peptide (Fig. 8, A and C). Next, we tested whether N-terminally truncated cathepsin V - due to usage of a second start codon - could explain the occurrence of cathepsin V in the nucleus. Indeed, the specific form of cathepsin V that we examined, i.e. cathepsin V that is N-terminally truncated at position 56, was sorted to the nuclei of Nthy-ori 3-1 cells, when expressed as a chimeric protein

with eGFP at its C-terminus (Fig 8, D). In stark contrast, the analogous specific form of cathepsins B, i.e. N-terminally truncated at position 52 and C-terminally tagged with eGFP, was not able to reach the nucleus (Fig. 8, B). This suggests that N-terminal truncation of any cysteine cathepsin does not inevitably lead to its nuclear localization. Moreover, nuclear localization of the N-terminally truncated cathepsin V form in its eGFP-tagged version was observed not only in Nthy-ori 3-1, but also in KTC-1 and HTh74 cells (Suppl. Fig. 1). The data highlight the principal ability of thyroid epithelial and carcinoma cell lines to generate and target a specific cathepsin V form to their nuclei.

3.7 Generation of stable thyroid cell lines expressing EGFP-tagged full-length and N-terminally truncated cathepsin V

Nthy-ori 3-1 cells were transduced to stably express h56NCV-eGFP, hereafter referred to as 'Nthyori-NCV'. As a control, we established the 'Nthyori-CV' cell line, which stably expresses hCV-eGFP. Both cellular models were analyzed by fluorescence microscopy (Fig. 9, A and B), revealing the expected localization of full-length and truncated cathepsin V, namely, full-length chimeric hCV-eGFP was excluded from the nuclei of Nthyori-CV cells (Fig. 9, A), while Nthyori-NCV cells exhibited a predominant nuclear localization of the N-terminally truncated h56NCV-eGFP chimeric protein (Fig. 9, B). It is noteworthy that the h56NCV-eGFP protein was localized in the nucleoplasm excluding the nucleoli and accumulating around chromosomes of dividing cells, while it was also present in the cytosol as obvious from the fluorescence pattern of the cytoplasm in which vesicular compartments are spared out as non-fluorescent regions (Fig. 9, B). These data are consistent with the results above for transiently expressing cells (see Fig. 8), demonstrating that the viral transduction as such does not change the trafficking pathway of eGFP-tagged full-length and N-terminally truncated cathepsin V in Nthy-ori 3-1 cells.

To assess the molecular masses of translated hCV-eGFP and h56NCV-eGFP chimeras, proteins of whole cell lysates of Nthyori-CV and Nthyori-NCV were separated by SDS-PAGE and immunoblotted with GFP-specific antibodies, while non-transduced Nthy-ori 3-1 cells were used as controls (Fig 9, C). The results showed anti-GFP positive bands in Nthyori-CV and Nthyori-NCV cells at approximately 64 kDa (Fig. 9, C, lane 2, arrow) and 57 kDa (Fig. 9, C, lane 3, dashed arrow), corresponding to the predicted molecular masses of hCV-eGFP and h56NCV-eGFP, respectively, whereas no anti-GFP positive bands were observed in non-transduced Nthy-ori 3-1 cells (Fig. 9, C, lane 1).

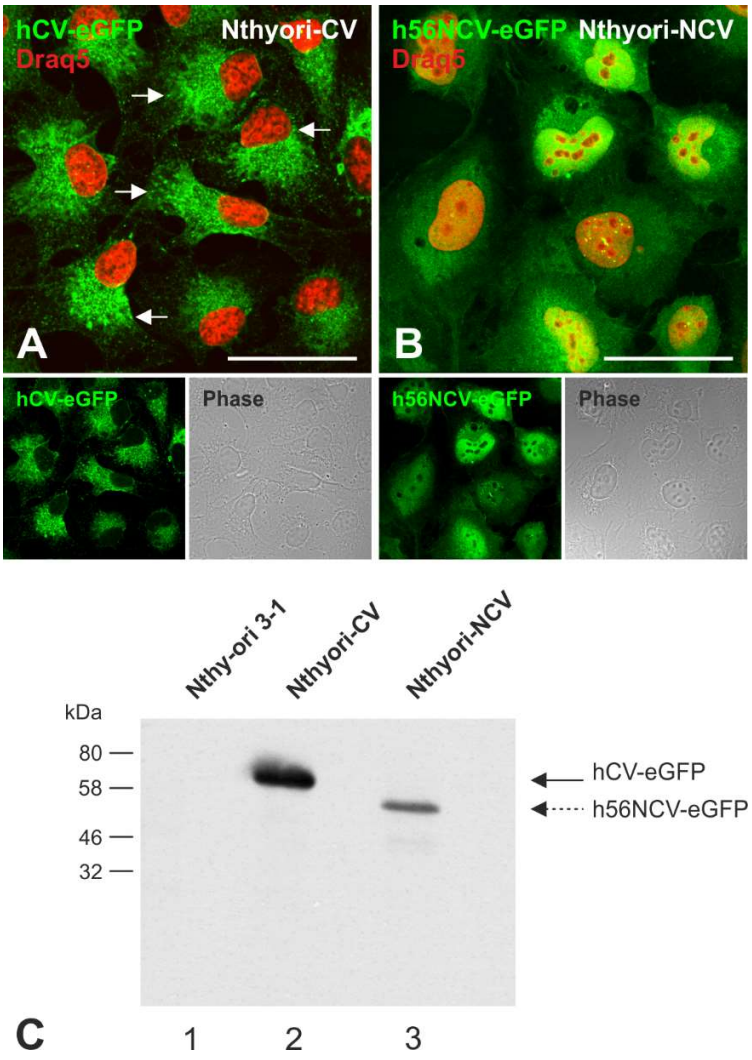

Figure 9: Transduced thyroid cell lines expressing eGFP-tagged full-length and N-terminally truncated cathepsin V. Confocal laser scanning micrographs of Nthyori-CV (A) and Nthyori-NCV cells (B) expressing eGFP-tagged full-length cathepsin V (hCV-eGFP) and N-terminally truncated cathepsin V (h56N-CV-eGFP), respectively, as indicated (green signals). The hCV-eGFP signals in Nthyori-CV cells were observed within reticular structures and in vesicles (arrows), while h56N-CV-eGFP was present within the cytoplasm and in nuclei of Nthyori-NCV cells (yellow signals in B as a result of overlapping green and red signals). Nuclei were counter-stained with Draq5 (red signals). Single channel fluorescence and corresponding phase contrast micrographs are depicted in bottom panels as indicated. Scale bars represent 50 µm. Whole cell lysates prepared from transduced Nthyori-CV and Nthyori-NCV cells were separated by 12.5% SDS-PAGE along with lysates from non-transduced Nthy-ori 3-1 cells used as a negative control (C). Immunoblotting with monoclonal mouse anti-GFP antibodies revealed bands at approximately 64 kDa (arrow) and 57 kDa (dashed arrow) as expected for the sizes of intact chimeric proteins hCV-eGFP and h56NCV-eGFP (lanes 2 and 3), respectively, indicating stability of the stably expressed chimeric proteins. Non-transduced control cells did not yield any immunopositive band (lane 1), indicating antibody specificity. Molecular mass markers are indicated in the left margins.

3.8 Expression levels of eGFP-tagged full-length and N-terminally truncated cathepsin V throughout the cell cycle

Because the immunofluorescence studies with non-transduced cells revealed endogenous cathepsin V to be highly expressed in S phase (see Fig. 6), we next investigated whether stable

expression of the eGFP-tagged chimeras with full-length (CV-eGFP) or N-terminally truncated (56NCV-eGFP) cathepsin V would alter their preferential expression in this phase of the cell cycle. Therefore, the stably expressing Nthyori-CV and Nthyori-NCV cells were synchronized in different cell cycle phases, and the levels of expression of hCV-eGFP and h56NCV-eGFP, respectively, were assessed using flow cytometry (Fig. 10). It was found that both full-length (Fig. 10, A and A') and N-terminally truncated cathepsin V (Fig. 10, B and B') were indeed significantly more abundant in S phase cells (green) in comparison to cultures arrested in G_0/G_1 (violet) and G_2/M phases (pale red). The expression levels in S phase (green) were comparable to those in non-synchronized Nthyori-CV or Nthyori-NCV cell cultures (Fig. 10, A' and B', grey bars), respectively.

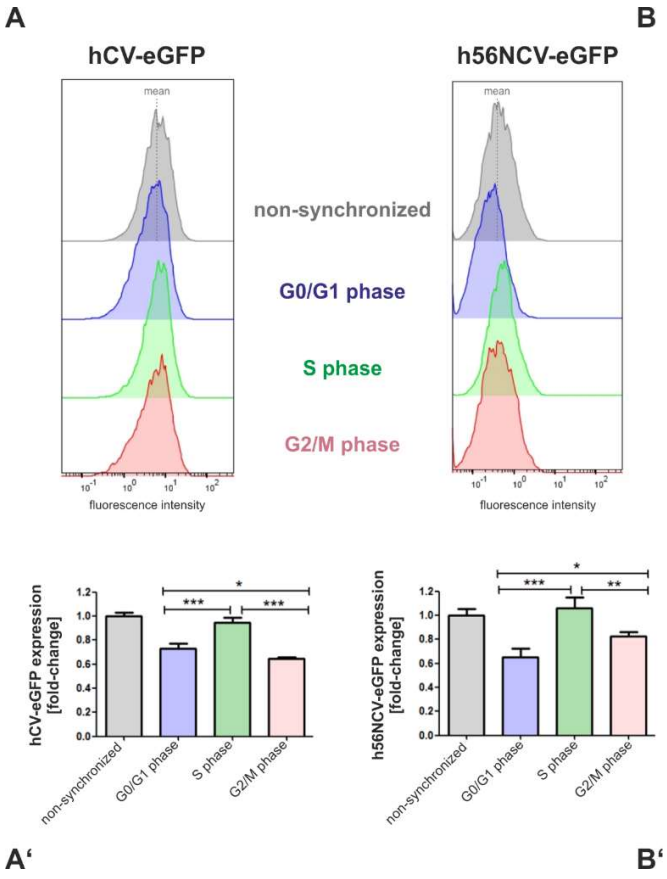

Figure 10: Analysis of expression levels of eGFP tagged full-length and N-terminally truncated cathepsin V in different phases of the cell cycle. Nthyori-CV (A and A') and Nthyori-NCV (B and B') cells were synchronized in different cell cycle phases as indicated and the levels of expression of hCV-eGFP and h56NCV-eGFP, respectively, were determined using flow cytometry. Representative examples of fluorescence intensity distributions are shown in the top panels (A and B), while quantitative results are plotted in the bottom panels (A' and B'). The graphs represent the fold-changes in expression levels of hCV-eGFP and h56NCV-eGFP in cells arrested at G_0/G_1 (violet), S (green), and G_2/M (pale red) phase, respectively, in comparison to non-synchronized cell cultures (grey). Data are depicted in bar charts as means + SD. Levels of significance were determined by one-way ANOVA and are indicated as * for $p < 0.05$, and *** for $p < 0.001$, respectively. The experiments were repeated three times. The dotted lines in A and B (grey panels) denote mean values equivalent to 1.0-fold.

3.9 Localization of eGFP-tagged full-length and N-terminally truncated cathepsin V throughout the cell cycle

As flow cytometry determines the amounts of total cellular cathepsin V, but does not allow conclusions on the localization of the proteins, we next asked where the hCV-eGFP and h56NCV-eGFP were localized throughout the cell cycle. Thus, Nthyori-NCV cells were arrested in G_0/G_1, S, and G_2/M phase, and compared to non-synchronized cell cultures by confocal laser scanning microscopy before subsequent quantification of the amounts of eGFP-derived fluorescence in the nuclei over the total cellular fluorescence (Fig. 11).

The results of imaging demonstrated once more that eGFP-tagged N-terminally truncated cathepsin V was localized to the nuclei of Nthyori-NCV cells in all cell cycle phases (Fig. 11, E-H), while full-length cathepsin V-eGFP chimeras was not detectable in the nuclei of Nthyori-CV cells in any cell cycle phase (Fig. 11, A-D). Interestingly, the proportion of nuclear h56NCV-eGFP was significantly higher in S phase-arrested Nthyori-NCV cells in comparison with non-synchronized controls or in cell cultures arrested in G_0/G_1 or G_2/M phase (Fig. 11, I), respectively. This supports the above findings by flow cytometry (see Fig. 10) and indicates that N-terminally truncated cathepsin V as an eGFP-tagged chimeric protein behaves like endogenous cathepsin V in terms of its predominant nuclear accumulation in S phase (see Fig. 6).

Therefore, the data strongly supports our proposal that there is an endogenous specific form of cathepsin V, which is N-terminally truncated at the second potential start site, i.e. methionine-56, that is targeted to the nuclei of thyroid epithelial cells where it is predominantly accumulating during S phase and might therefore play a prominent role in the progression of late stages of the cell cycle. These findings further indicated that the established cell lines Nthyori-CV and Nthyori-NCV represent valuable cellular models to study the role of nuclear cathepsin V in more detail, and to identify potential substrates which is however beyond this study.

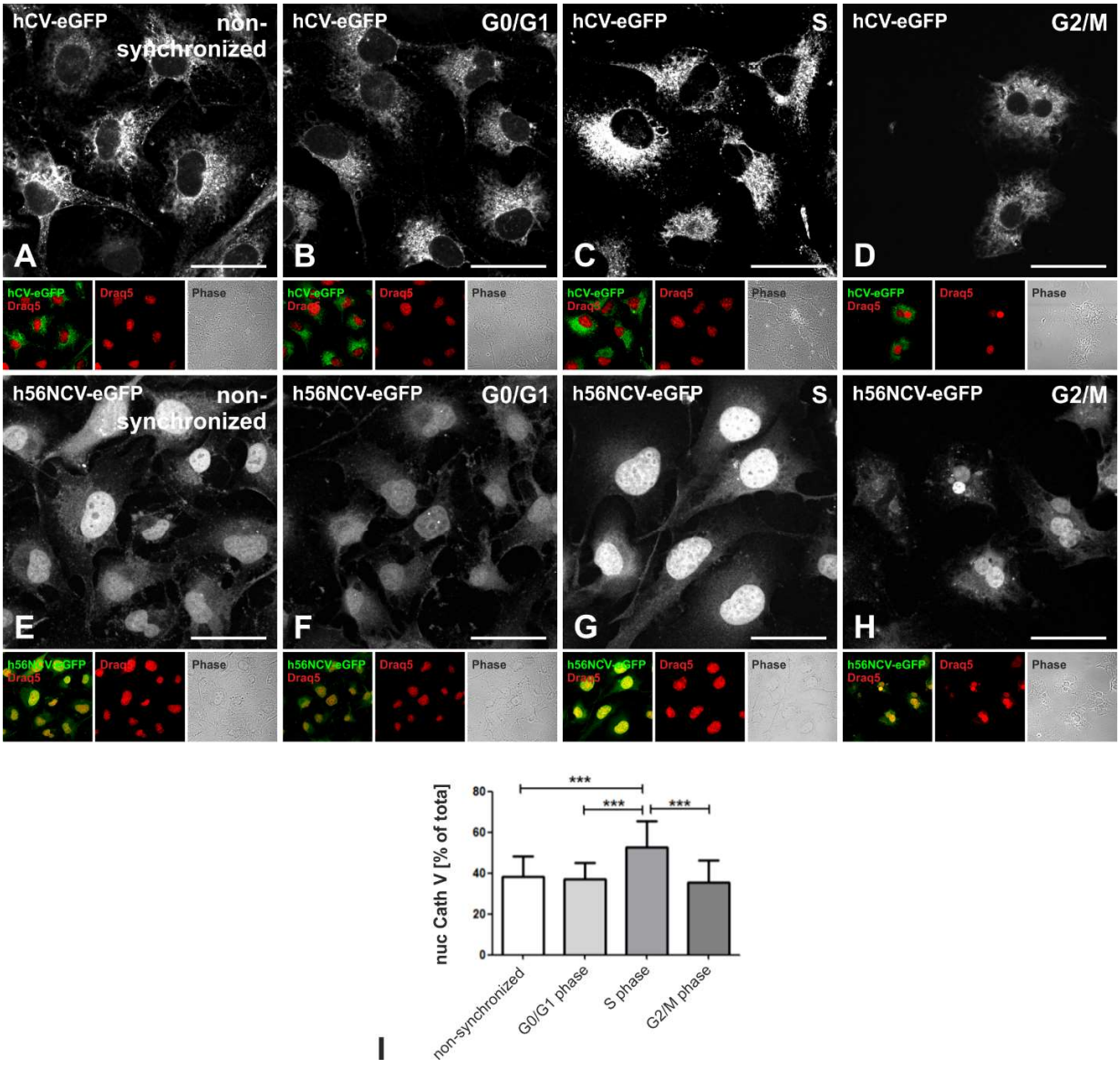

Figure 11: Localization of eGFP-tagged full-length and N-terminally truncated cathepsin V throughout the cell cycle. Localization of hCV-eGFP and h56NCV-eGFP was studied in transduced Nthyori-CV (A-D) and Nthyori-NCV cells (E-H), respectively. Cells were synchronized in different cell cycle stages, i.e. G_0/G_1 (B and F), S (C and G), and G_2/M phase (D and H), and compared to non-synchronized cell cultures (A and E). Confocal laser scanning micrographs depict eGFP-derived fluorescence signals (top panels) in reticular structures of PFA-fixed and Draq5 counter-stained hCV-eGFP expressing cells (A-D) and predominantly within nuclei of h56NCV-eGFP expressing cells (E-H). Single channel, merged and corresponding phase contrast micrographs are depicted in the bottom panels as indicated. Scale bars represent 50 µm. Micrographs of Nthyori-NCV cells were analyzed using Cell Profiler to quantify the percentages of nuclear over total cellular GFP signals. Data are depicted in bar charts (I) as means + SD. At least 70 cells were analyzed per each cell cycle phase and compared to non-synchronized cells. Levels of significance were determined by one-way ANOVA followed by Tukey *post hoc* test and indicated as *** for $p < 0.001$.

3.10 Expression of eGFP-tagged N-terminally truncated cathepsin V results in hyperproliferation of Nthyori-NCV cells

In order to test whether the N-terminally truncated form of cathepsin V is potentially directly involved in initiating cell proliferation, we first sought to determine the metabolic activity and proliferation rates of transduced cells expressing N-terminally truncated cathepsin V (Nthyori-NCV) *versus* the transduced cells expressing full-length cathepsin V (Nthyori-CV) and non-transduced thyroid epithelial cells (Nthy-ori 3-1) by an MTT assay. The results showed that MTT reduction was significantly higher in Nthyori-NCV cells in comparison to Nthyori-CV and non-transduced Nthy-ori 3-1 cells, while there was no difference in MTT-conversion rates between Nthyori-CV and Nth-yori 3-1 cells (Fig. 12, A). To verify that the increase in MTT reduction by Nthyori-NCV cell cultures is indeed indicative of enhanced cell proliferation rates due to the expression of the N-terminally truncated and nuclear targeted cathepsin V form, and not a mere induction of metabolic activity, the same numbers of Nthyori-NCV, Nthyori-CV, and Nthy-ori 3-1 cells were seeded and cultured for up to three days, while they were counted every day after seeding. We found that the numbers of Nthyori-NCV cells (Fig. 12, B, closed dots) were higher than those of Nthyori-CV (closed squares) and Nthy-ori 3-1 cell cultures (open squares) at all time intervals investigated (Fig 12, B). These data strongly support the notion that it is proliferation which correlates with the expression of nuclear cathepsin V forms.

Since we found that Nthyori-NCV cells were more proliferative than Nthy-ori 3-1 and Nthyori-CV cells, next, we investigated how the cell lines respond to a lack of growth factors, i.e., in particular, whether they are in proliferative or quiescent states after serum depletion. For this purpose, sub-confluent Nthy-ori 3-1, Nthyori-CV, and Nthyori-NCV cell cultures were serum-starved for 48 h and immunolabeled with monoclonal antibodies against the proliferation marker Ki67 (Fig 12, C1-C3). Confocal images were analyzed by Cell Profiler to determine proliferation rates of cells as proportion of Ki67-positive cells among total number of cells as well as to quantify the intensity of Ki67 immunostaining. The results revealed that 90% of starved Nthyori-NCV exhibited Ki67-positive signals (Fig 12, D, dark grey bar), indicating that most of the cells remained in a proliferative state despite growth factor deprivation. On the other hand, approx. 50% of starved Nthy-ori 3-1 and Nthyori-CV were Ki67 positive (Fig. 12, D, white and light grey bars, respectively), indicating that serum starvation for 48 h induced cells to exit the cell cycle and enter the resting G_0 phase. In addition, the intensity of Ki67 immunostaining, representing the amounts of Ki67 expression, was significantly higher in Nthyori-NCV in comparison to Nthy-ori 3-1 and Nthyori-CV (Fig. 12, E). These findings imply that nuclear N-terminally truncated cathepsin V promotes cell cycle progression, possibly through affecting the passing of transit checkpoints.

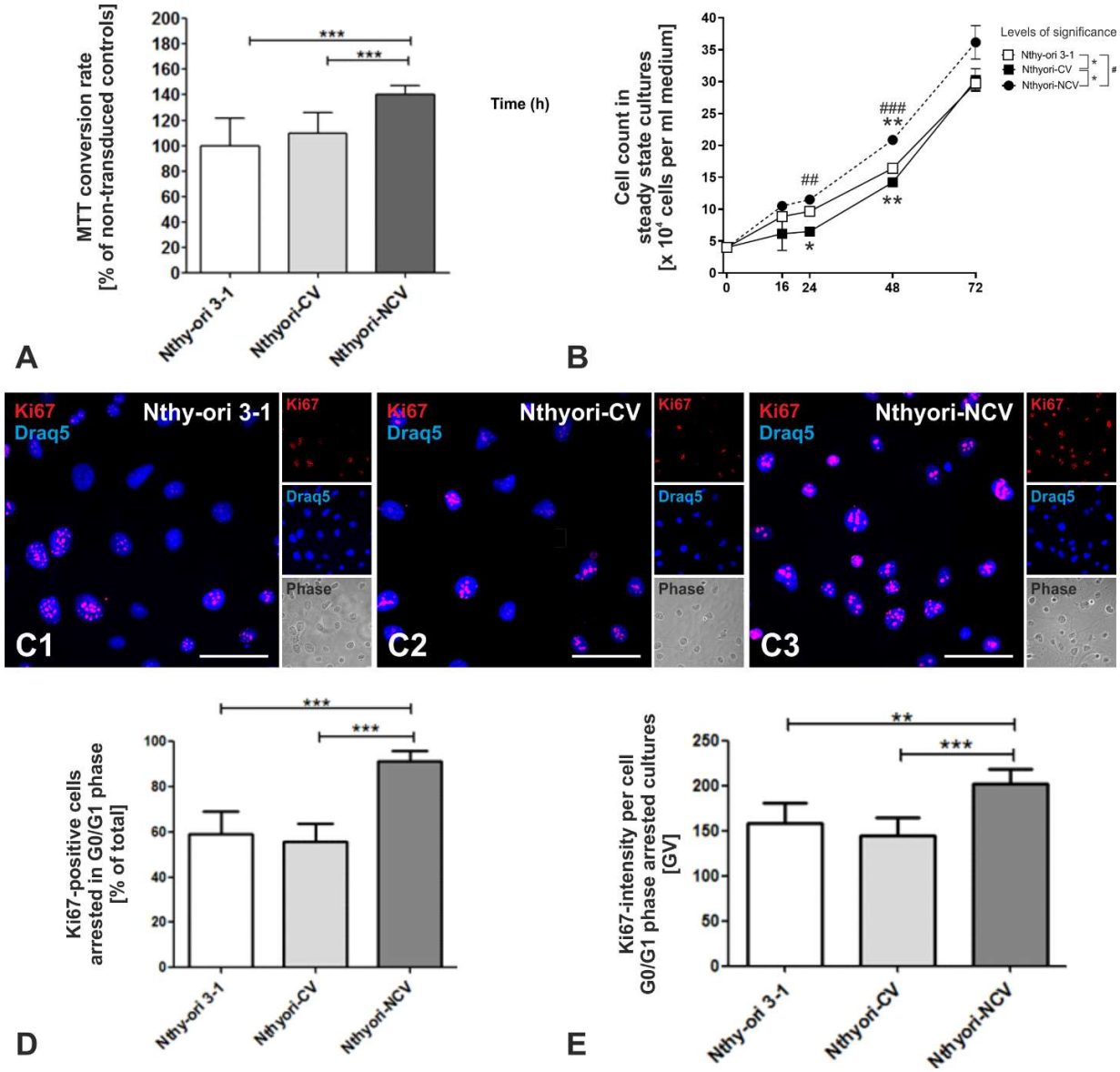

Figure 12: Effects of stable expression of eGFP-tagged full-length and N-terminally truncated cathepsin V on proliferation of Nthy-ori 3-1 cells. (A) The MTT assay was used to determine the cell numbers and metabolic activities of transduced cells, namely Nthyori-CV (light grey) and Nthyori-NCV (dark grey) in comparison to non-transduced Nthy-ori 3-1 cells (open bar). Values are expressed as percentages of non-transduced Nthy-ori 3-1 cells. Data represent the means + SD of three independent experiments with four replicates each. **(B)** Growth curves of Nthy-ori 3-1 (open squares), Nthyori-CV (filled squares), and Nthyori-NCV cultures (filled dots, dashed line), as indicated, were generated using 4,000 cells initially seeded in 6-well plates. At the indicated time, cells were *trypsinized and counted with a hemocytometer.* Data represent the means ± SD of two independent experiments with three replicates each. **(C)** Confocal laser scanning micrographs of Nthy-ori 3-1 (C1), Nthyori-CV (C2), and Nthyori-NCV cells (C3) upon serum-starvation for 48 h and immunolabeling with antibodies against Ki67 (red signals) and counter-staining of nuclear DNA with Draq5 (blue signals). Merged, single-channel fluorescence and corresponding phase contrast micrographs are depicted as indicated. Scale bars represent 50 µm. **(D)** Proliferation rates of serum-starved cells were determined as percentages of Ki67-positive cells among all Draq5-positive cells for at least 400 cells, each, respectively. **(E)** Intensity of Ki-67 immunostaining was normalized to the total numbers of cells and values are given as means + SD. Levels of significance were determined by one-way ANOVA followed by Tukey *post hoc* test and are indicated as ** for $p < 0.01$, and *** for $p < 0.001$.

4. Discussion

The data presented in this study provides evidence for a direct role of an N-terminally truncated nuclear cathepsin V form in the regulation of cell cycle progression of thyroid epithelial and carcinoma cells. We further propose that nuclear cysteine cathepsin V might serve as a potential future biomarker of thyroid carcinoma. In addition, nuclear cathepsin V expression is correlated with deregulation of cell proliferation and hence, it contributes to promoting carcinogenesis and/or thyroid cancer progression. Thus, it will be important to determine the substrates of the nuclear cathepsin V forms in thyroid cells. Such an endeavor will be possible to tackle in future since we have now established stably expressing thyroid cell lines in which the effects of expressed N-terminally truncated cathepsin V forms become approachable in comparison to full-length cathepsin V, which is not sorted to the nucleus.

4.1 The importance of cysteine cathepsins for the thyroid gland

The cysteine cathepsins B, K, L, and S are important for maintaining proper thyroid function because they are involved in proteolytic processing and degradation of the prohormone thyroglobulin for thyroid hormones liberation [17, 29]. Therefore, alterations in the expression levels and/or localization of any of these proteases can contribute to establishing or worsening of thyroid disorders including cancer. For instance, overexpression of cathepsin S was reported to be associated with lymph node metastasis and poor prognosis in PTC [30]. Several studies highlighted that cathepsin B is mislocalized towards the basolateral pole of cells in PTC, indicating that cathepsin B could possibly promote thyroid cancer cell invasion through enabling excessive extracellular matrix (ECM) degradation [6, 7, 11]. In this study, we detected cathepsin B to some extent in the nuclei of thyroid cancer tissue cells. However, immunofluorescence analyses of this study revealed that cathepsin V is a lot more prevalent in the nuclei of cells in cold nodules, PTC and FTC tissue in comparison to cathepsin B and when compared with non-cancerous thyroid tissues, i.e. hot nodules and thyroid goiter tissue, where only few cells feature nuclear cathepsin V.

These results suggested cathepsin V could be used as a potential biomarker in the diagnosis of thyroid cancer, which is the most frequent cancer type of the endocrine system and responsible for most deaths from endocrine cancers [31]. Thus far, among the endo-lysosomal proteases, the aspartic cathepsin D was found to be overexpressed in thyroid cancer and proposed to allow distinguishing PTC and FTC from non-cancerous tissue [32, 33]. It is important to identify more suitable biomarkers of thyroid cancer, because the majority of thyroid nodules are benign, and only a small proportion of approx. 5% are malignant [34]. Therefore, distinguishing malignant from benign nodules is crucial for an appropriate treatment and follow-up. At present, fine needle

aspiration biopsy (FNAB) is a diagnostic tool considered the gold standard to differentiate malignant from benign thyroid nodules [35]. However, 10-15% of the biopsies cannot be diagnosed due to a lack of specific biomarkers classifying them as suspicious for developing into malignant lesions. In such cases, the patients undergo diagnostic thyroid lobectomy, although in most cases the tissue turns out to be benign [36-39]. Therefore, there is an urgent need for novel biomarkers of thyroid cancer in order to resolve this diagnostic dilemma. At the same time, such thyroid cancer biomarkers could help to avoid unnecessary surgery.

It is worth mentioning that elevated levels of cathepsin V expression are part of a new diagnostic molecular test panel for breast cancer [40]. Several studies have demonstrated the overexpression of cathepsin V (also known as cathepsin L2) in various other types of human cancers. For instance, transcript levels of cathepsin V are significantly increased in endometrial cancer, particularly in poorly differentiated G3 tumors, suggesting that cathepsin V might be involved in the progression of this cancer type [41]. The elevated expression of cathepsin V is correlated with poor prognosis also in hepatocellular carcinoma [40, 42, 43]. Cathepsin V is also highly expressed in colorectal, ovarian, renal and squamous cell carcinomas [43, 44]. Therefore, mechanistic studies on the roles of cathepsin V in epithelial and carcinoma cell biology are timely and urgent.

4.2 Characterization of *in vitro* models

The hallmarks of cancer encompass EMT, i.e. the downregulation of epithelial markers like claudin-1, E-cadherin and occludin in parallel with upregulation of mesenchymal markers like vimentin [45-48]. Our experiments therefore were first devoted to characterizing the cell lines used in this study, i.e. Nth-yori 3-1, KTC-1, and HTh74, with respect to their epithelial and mesenchymal features. The results revealed that these cell lines are representative models of different stages of EMT. The thyroid cell lines KTC-1 and HTh74 harbor different oncogenic mutations [49, 50]. KTC-1 demonstrated the most epithelial-like features, while HTh74 cells exhibited mesenchymal properties. Since HTh74 cells are derived from ATC, the most aggressive type of thyroid cancer, it comes without surprise that these cells were most dedifferentiated in comparison to the other cell lines. KTC-1 cells are derived from a patient with PTC, the most common and often curable type of thyroid cancer, which is in line with our findings that these cells maintain epithelial features to quite some extent. In contrast, Nthy-ori 3-1 is the only cell line presently available that is derived from normal human thyroid tissue. It was immortalized using the simian virus 40 (SV40). Although Nthy-ori 3-1 cells are non-tumorigenic in nude mice, our results showed that they possess mesenchymal characteristics most likely due to the immortalization process which mediates neoplastic transformation of epithelial cells. SV40 induces immortalization by inactivating tumor

suppressor genes such as p53, retinoblastoma and others, leading to continuous proliferation of cells beyond their otherwise limited life span up to the Hayflick limit [51, 52].

4.3 Establishing a stable cell line expressing GFP-tagged nuclear cathepsin V

Since our results showed that cathepsin V is more abundant than cathepsin B in the nuclei of thyroid epithelial and carcinoma cells *in situ* and *in vitro*, we focused our further studies on nuclear cathepsin V with the aim to understand its site of synthesis and trafficking route. Using specific antibodies against the pro-peptide of cathepsin V (CV55-1C5), we showed that procathepsin V is not localized to the nuclei of thyroid epithelial and carcinoma cells. These data imply that nuclear cathepsin V could either have escaped as the mature enzyme from endo-lysosomes due to leakiness of their limiting membranes, or, alternatively, nuclear cathepsin V represents an N-terminally truncated form of the enzyme that enters the nucleus upon translation in the cytosol. The findings of this study therefore contrast a previous study of our group on colorectal carcinoma cells, in which full-length cathepsin L reached their nuclei [25]. Hence, different forms of cysteine cathepsins can be sorted to the nuclear compartment based on the type of cysteine cathepsin itself and on the specific cell or tissue type. Collectively, however, the findings of this and previous studies imply that nuclear cysteine cathepsins are critically involved in tumorigenesis through the proteolytic processing of specific substrates.

However, this study was conducted because detection methods based on antibodies do not conclusively allow to discriminate between leaky lysosome-derived or cytosolically translated cathepsin V forms. Hence, to identify which form of cathepsin V can reach the nucleus, in principle, we examined the localization of full-length (CV-eGFP) and N-terminally truncated cathepsin V (56NCV-eGFP) expressed in the thyroid cell lines as chimeric proteins tagged with EGFP. We found that it is the N-terminally truncated cathepsin V which becomes localized in the nucleus of thyrocytes in a pattern closely resembling endogenous cathepsin V. In stark contrast, full-length cathepsin V follows the classical trafficking pathway of endo-lysosomal proteases and it did not reach the nucleus, even not under stressful conditions such as cell cycle blockage. Interestingly, this study shows also that N-terminally truncated cathepsin B (52NCB-eGFP) does not reach the nuclei of Nthy-ori 3-1 cells. This is important to note because studies conducted by the Baici group reported that N-terminally truncated forms of cysteine cathepsins can be sorted to cellular compartments other than the nucleus, namely, exon-skipped transcripts of cathepsin B result in mitochondrial import of the translated protein [53]. Thus, taken together, our previous and the results of this study led us to conclude that the mere lack of the pre-peptide of a cysteine cathepsin does not explain its entry into the nucleus. This study indicates that trafficking to the nucleus is a

specific feature for N-terminally truncated cathepsin V in thyroid epithelial cells that bear mutational alterations eventually leading to a neoplastic phenotype.

4.4 Significance of nuclear cysteine cathepsin V in thyroid cell proliferation

We were further interested to investigate the potential function of N-terminally truncated cathepsin V in the nuclei of thyroid epithelial cells, and examined the consequences of its expression in Nthy-ori 3-1 cells. For this purpose, we generated two transduced cell lines, namely Nthyori-CV and Nthyori-NCV cells expressing eGFP tagged full-length (CV-eGFP) and N-terminally truncated (56NCV-eGFP) cathepsin V, respectively. Nthyori-CV cells served as an internal control for the viral transduction and stable expression of an eGFP-tagged cathepsin V-chimera. Because CV-eGFP followed the expected transport pathway and since the Nthyori-CV cells showed no obvious phenotypic changes, we concluded that the method of lentiviral transduction as such was tolerated well by the Nthy-ori 3-1 cell line. Regarding the localization and expression pattern of N-terminally truncated cathepsin V in Nthyori-NCV, we found that 56NCV-eGFP is predominantly localized in the nuclei and its expression is highest during S phase of the cell cycle. This verified that the stably expressed nuclear form of cathepsin V, i.e. 56NCV-eGFP, behaves similar to endogenous nuclear cathepsin V. Further on, we relied on the transduced Nthyori-NCV cellular model to study whether expression of N-terminally truncated cathepsin V (the nuclear form) affects proliferation of thyrocytes by comparing them to non-transduced control cells (Nthy-ori 3-1) and full-length cathepsin V expressing Nthyori-CV cells.

The results of this study, obtained from MTT assays, cellular growth curve determinations and Ki67 expression studies, demonstrated collectively that Nthyori-NCV cells are indeed more proliferative than Nthy-ori 3-1 and Nthyori-CV cells. These findings led us to conclude that 56NCV-eGFP induces cell cycle progression of thyroid epithelial cells with neoplastic features such as Nthy-ori 3-1 cells. To commit for entry into a new cell cycle and become proliferative, cells must pass the restriction point at the G1/S transition phase, which ensures the availability of adequate growth factors and nutrients. Normal cells require growth factors to promote G1 to S phase transition and thereby withdrawal of growth factors leads to cell cycle arrest at G1 phase and ultimately to the exit from the cell cycle in order to enter a quiescent state (G0 phase). However, cancer cells lose the dependence on growth factors due to altered growth factor receptors and because of deregulation of restriction points. Hence, they can commit to S phase entry and continue progressing through the cell cycle, regardless of the availability of growth factors or essential nutrients, leading to uncontrolled cell proliferation. Based on the expression of the Ki67 proliferation marker, we found that expression of nuclear N-terminally truncated cathepsin V results in reduced responsiveness of the Nthyori-NCV cells to nutrient deprivation in

comparison to both, the Nthy-ori 3-1 parent cell line and the Nthyori-CV cells used as controls for the viral transduction. This data has further strengthened our conviction that nuclear cathepsin V is associated with cell cycle deregulation leading to hyperproliferation and, consequently, promotion of thyroid tumorigenesis.

4.5 Molecular mechanistic functions of nuclear cysteine cathepsins in cancer cell cycle progression

Cysteine cathepsins are known to drive cancer progression mainly due to their secretion into extracellular space where they are involved in degradation of cell-cell junction proteins like E-cadherin, and extracellular matrix (ECM) constituents like collagen type IV and laminin, thereby paving the way for tumor cell migration and invasion [6, 8, 11, 30, 44, 54, 55]. However, the appearance of cysteine cathepsins in the nuclei of carcinoma cells highlighted a new dimension and molecular mechanism underlying the roles of cathepsins in cancer progression.

It was found that the transcription factor Snail can promote nuclear localization of cathepsin L in breast and prostate cancer cells, leading to enhanced processing of CUX1 which, in turn, represses E-cadherin expression and subsequently promotes EMT [56]. In a previous study, our group reported the presence of cathepsin L, the closest homologue of cathepsin V, in the nuclei of colorectal carcinoma cells (HCT116). It was observed that the inhibition of cathepsin L activity slows down cell cycle progression of HCT116, whereas over-expression of cathepsin L accelerates S-phase entry [25]. Since we have reported previously that cathepsin L is not present in the nuclei of thyrocytes, we propose that it is not cathepsin L, but its closest relative cathepsin V, that seems to play a prominent role in thyroid carcinoma as indicated by the results of our present study. We believe that this observation is important because cathepsin V localizes to the nuclei of thyrocytes, both *in situ* and *in vitro*. Since the sub-nuclear localization of cathepsin V is similar in thyroid carcinoma tissue cells and in thyroid carcinoma cell lines and in the herein established cellular model Nthyori-NCV, cathepsin V most possibly involves in thyroid tumorigenesis through interaction with nuclear proteins to then deregulate cell cycle progression of thyrocytes.

Obvious questions arise, namely, what is the precise role of nuclear cathepsin V in thyroid carcinoma cells, when in the cell cycle does it act, and what are its interaction partners and possible substrates in the nucleus. While these questions are beyond the present investigation, it is interesting to note that the results achieved by our group are in accordance with several other studies, which described correlations between the expression of cathepsin V and cell cycle progression [3]. It was shown that MENT, an effective inhibitor of the cathepsins L and V, accumulates in the nucleus, where it might block cell proliferation through direct interaction with a

nuclear cysteine protease in a nucleosome-guided pathway [57]. In addition, cathepsin V silencing has been shown to exert cell type-specific effects on the growth of breast cancer cell lines, i.e. cathepsin V siRNA inhibits the growth of MCF7 cells, but stimulates the growth of SKBR3 cells [58]. Expression of cathepsin V is significantly correlated with that of different growth regulatory genes such as Ki-67, cyclin B1, MYBL2, p21/WAF, and HER2 receptor tyrosine kinase in endometrial cancer [41]. Taken together, these findings corroborate the proposed function of nuclear cysteine cathepsins – including cathepsin V - in cell cycle regulation. Here, we found that the thyroid epithelial and carcinoma cell lines Nthy-ori 3-1, KTC-1, and HTh-74 exhibited the highest amounts of intra-nuclear detectable cathepsin V in S phase-arrested cells. These findings support our notion that nuclear cathepsin V plays a potential role in cell cycle progression specifically during S phase of thyroid cells.

Interestingly, it has been found that the E2 promoter binding factor 1 (E2F1), a transcription factor, induces expression of cathepsin V by binding directly to its promoter [59]. E2F1 plays a fundamental role in cell cycle regulation by activating the transcription of genes required for DNA replication and, hence, is important for exit of G1 phase and S phase entry [60, 61]. E2F1 has also been associated with oncogenic functions, because it induces abnormal cell proliferation in different types of cancer including thyroid cancer [62-64]. Furthermore, it has been found that E2F1 is upregulated in PTC and ATC, where it acts as an inducer of tumor cell proliferation [65]. Hence, we propose that overexpression of E2F1 in thyroid cancer might result in upregulation of cathepsin V expression, including that of an N-terminally truncated form that enters the nucleus and can then further promote proliferation of thyroid cells in a self-sustained cycle. Future studies are underway to analyze this hypothesis in detail and to proof an interconnected deregulation of cell cycle progression in dependence of co-expression of E2F1 and nuclear cathepsin V in thyroid cancer.

5. Acknowledgements

This study was supported by the Deutscher Akademischer Austauschdienst (DAAD), Research Grants – Doctoral Programmes in Germany, PRNo. 91534725 to AAH. Further funding was provided by Jacobs University Bremen, Germany, Project 6113/90140, to AAH and KB. The study was further supported by Deutsche Forschungsgemeinschaft, Bonn, Germany, in the framework of the FOR367, BR 1308/6-1 and 6-2 to KB. The authors are indebted to Maren Rehders (Jacobs University Bremen, Germany) for excellent technical assistance. We are grateful to Dr. Junichi Kurebayashi (Kawasaki Medical School, Okayama, Japan) and Dr. Nils-Erik Heldin (Uppsala University, Sweden) for kindly sharing the KTC-1 and HTh74 cell lines, respectively.

6. Author contributions

All authors contributed to the study conception and design. Material preparation, data collection and analysis were performed by AAH, VV, NSe, ST, AMP, ZH, EW, DF, REB and KB. The first draft of the manuscript was written by AAH and KB, and all authors commented on previous versions of the manuscript. All authors read and approved the final manuscript.

7. References

[1] N.D. Rawlings, A.J. Barrett, P.D. Thomas, X. Huang, A. Bateman, R.D. Finn, The MEROPS database of proteolytic enzymes, their substrates and inhibitors in 2017 and a comparison with peptidases in the PANTHER database, Nucleic Acids Res 46(D1) (2018) D624-d632.

[2] K. Brix, A. Dunkhorst, K. Mayer, S. Jordans, Cysteine cathepsins: cellular roadmap to different functions, Biochimie 90(2) (2008) 194-207.

[3] K. Brix, J. McInnes, A. Al-Hashimi, M. Rehders, T. Tamhane, M.H. Haugen, Proteolysis mediated by cysteine cathepsins and legumain-recent advances and cell biological challenges, Protoplasma 252(3) (2015) 755-74.

[4] K. Brix, M. Linke, C. Tepel, V. Herzog, Cysteine proteinases mediate extracellular prohormone processing in the thyroid, Biol Chem 382(5) (2001) 717-25.

[5] K. Brix, J. Szumska, J. Weber, M. Qatato, V. Venugopalan, A. Al-Hashimi, M. Rehders, Auto-Regulation of the Thyroid Gland Beyond Classical Pathways, Exp Clin Endocrinol Diabetes (2020).

[6] S. Shuja, M.J. Murnane, Marked increases in cathepsin B and L activities distinguish papillary carcinoma of the thyroid from normal thyroid or thyroid with non-neoplastic disease, Int J Cancer 66(4) (1996) 420-6.

[7] S. Shuja, J. Cai, C. Iacobuzio-Donahue, J. Zacks, R.M. Beazley, J.M. Kasznica, C.J. O'Hara, R. Heimann, M.J. Murnane, Cathepsin B activity and protein levels in thyroid carcinoma, Graves' disease, and multinodular goiters, Thyroid 9(6) (1999) 569-77.

[8] S. Tedelind, K. Poliakova, A. Valeta, R. Hunegnaw, E.L. Yemanaberhan, N.E. Heldin, J. Kurebayashi, E. Weber, N. Kopitar-Jerala, B. Turk, M. Bogyo, K. Brix, Nuclear cysteine cathepsin variants in thyroid carcinoma cells, Biol Chem 391(8) (2010) 923-35.

[9] O.V. Kalinichenko, T.M. Myshunina, M.D. Tron'ko, [Changes in active cysteine cathepsins in lysosomes from tissues thyroid papillary carcinomas with various biological characteristics], Fiziol Zh 59(5) (2013) 11-9.

[10] C. Srisomsap, P. Subhasitanont, A. Otto, E.C. Mueller, P. Punyarit, B. Wittmann-Liebold, J. Svasti, Detection of cathepsin B up-regulation in neoplastic thyroid tissues by proteomic analysis, Proteomics 2(6) (2002) 706-12.

[11] S. Tedelind, S. Jordans, H. Resemann, G. Blum, M. Bogyo, D. Führer, K. Brix, Cathepsin B trafficking in thyroid carcinoma cells, Thyroid Res 4 Suppl 1(Suppl 1) (2011) S2.

[12] E.M. Duncan, T.L. Muratore-Schroeder, R.G. Cook, B.A. Garcia, J. Shabanowitz, D.F. Hunt, C.D. Allis, Cathepsin L proteolytically processes histone H3 during mouse embryonic stem cell differentiation, Cell 135(2) (2008) 284-94.

[13] A. Pišlar, M. Perišić Nanut, J. Kos, Lysosomal cysteine peptidases - Molecules signaling tumor cell death and survival, Semin Cancer Biol 35 (2015) 168-79.

[14] J. Reiser, B. Adair, T. Reinheckel, Specialized roles for cysteine cathepsins in health and disease, J Clin Invest 120(10) (2010) 3421-31.

[15] S.M. Soond, M.V. Kozhevnikova, P.A. Townsend, A.A. Zamyatnin, Jr., Cysteine Cathepsin Protease Inhibition: An update on its Diagnostic, Prognostic and Therapeutic Potential in Cancer, Pharmaceuticals (Basel) 12(2) (2019).

[16] Z. Wang, Z. Xiang, T. Zhu, J. Chen, M.Z. Zhong, J. Huang, K.S. Wang, L. Li, L.Q. Sun, W.B. Zhou, Cathepsin L interacts with CDK2-AP1 as a potential predictor of prognosis in patients with breast cancer, Oncol Lett 19(1) (2020) 167-176.

[17] B. Friedrichs, C. Tepel, T. Reinheckel, J. Deussing, K. von Figura, V. Herzog, C. Peters, P. Saftig, K. Brix, Thyroid functions of mouse cathepsins B, K, and L, J Clin Invest 111(11) (2003) 1733-45.

[18] H. Büth, Contribution of the lysosomal cysteine protease cathepsin B to extracellular matrix remodeling during keratinocyte migration and wound healing, http://www.jacobs-university.de/phd/files/1146557428.pdf, 2006.

[19] H. Hanenberg, X.L. Xiao, D. Dilloo, K. Hashino, I. Kato, D.A. Williams, Colocalization of retrovirus and target cells on specific fibronectin fragments increases genetic transduction of mammalian cells, Nat Med 2(8) (1996) 876-82.

[20] Z. Hein, H. Uchtenhagen, E.T. Abualrous, S.K. Saini, L. Janßen, A. Van Hateren, C. Wiek, H. Hanenberg, F. Momburg, A. Achour, T. Elliott, S. Springer, D. Boulanger, Peptide-independent stabilization of MHC class I molecules breaches cellular quality control, J Cell Sci 127(Pt 13) (2014) 2885-97.

[21] A. Halenius, S. Hauka, L. Dölken, J. Stindt, H. Reinhard, C. Wiek, H. Hanenberg, U.H. Koszinowski, F. Momburg, H. Hengel, Human cytomegalovirus disrupts the major histocompatibility complex class I peptide-loading complex and inhibits tapasin gene transcription, J Virol 85(7) (2011) 3473-85.

[22] J. Szumska, Z. Batool, A. Al-Hashimi, V. Venugopalan, V. Skripnik, N. Schaschke, M. Bogyo, K. Brix, Treatment of rat thyrocytes in vitro with cathepsin B and L inhibitors results in disruption of primary cilia leading to redistribution of the trace amine associated receptor 1 to the endoplasmic reticulum, Biochimie 166 (2019) 270-285.

[23] K. Krause, S. Karger, S.Y. Sheu, T. Aigner, R. Kursawe, O. Gimm, K.W. Schmid, H. Dralle, D. Fuhrer, Evidence for a role of the amyloid precursor protein in thyroid carcinogenesis, J Endocrinol 198(2) (2008) 291-9.

[24] L. Kamentsky, T.R. Jones, A. Fraser, M.A. Bray, D.J. Logan, K.L. Madden, V. Ljosa, C. Rueden, K.W. Eliceiri, A.E. Carpenter, Improved structure, function and compatibility for CellProfiler: modular high-throughput image analysis software, Bioinformatics 27(8) (2011) 1179-80.

[25] T. Tamhane, R. Lllukkumbura, S. Lu, G.M. Maelandsmo, M.H. Haugen, K. Brix, Nuclear cathepsin L activity is required for cell cycle progression of colorectal carcinoma cells, Biochimie 122 (2016) 208-18.

[26] V. Neuhoff, K. Philipp, H.G. Zimmer, S. Mesecke, A simple, versatile, sensitive and volume-independent method for quantitative protein determination which is independent of other external influences, Hoppe Seylers Z Physiol Chem 360(11) (1979) 1657-70.

[27] P. Guillaud, J. Vermont, D. Seigneurin, Automatic classification of cells in cell cycle phases based on Ki-67 antigen quantification by fluorescence microscopy, Cell Prolif 24(5) (1991) 481-91.

[28] X. Sun, P.D. Kaufman, Ki-67: more than a proliferation marker, Chromosoma 127(2) (2018) 175-186.

[29] S. Jordans, S. Jenko-Kokalj, N.M. Kühl, S. Tedelind, W. Sendt, D. Brömme, D. Turk, K. Brix, Monitoring compartment-specific substrate cleavage by cathepsins B, K, L, and S at physiological pH and redox conditions, BMC Biochem 10 (2009) 23.

[30] J. Tan, X. Qian, B. Song, X. An, T. Cai, Z. Zuo, D. Ding, Y. Lu, H. Li, Integrated bioinformatics analysis reveals that the expression of cathepsin S is associated with lymph node metastasis and poor prognosis in papillary thyroid cancer, Oncol Rep 40(1) (2018) 111-122.

[31] L.C. Moeller, D. Führer, Thyroid hormone, thyroid hormone receptors, and cancer: a clinical perspective, Endocr Relat Cancer 20(2) (2013) R19-29.

[32] J.L. Kraimps, T. Métayé, C. Millet, D. Margerit, P. Ingrand, J.M. Goujon, P. Levillain, P. Babin, F. Begon, J. Barbier, Cathepsin D in normal and neoplastic thyroid tissues, Surgery 118(6) (1995) 1036-40.

[33] N.M. Paricharttanakul, K. Saharat, D. Chokchaichamnankit, P. Punyarit, C. Srisomsap, J. Svasti, Unveiling a novel biomarker panel for diagnosis and classification of well-differentiated thyroid carcinomas, Oncol Rep 35(4) (2016) 2286-96.

[34] T. Carling, R. Udelsman, Thyroid cancer, Annu Rev Med 65 (2014) 125-37.

[35] J. Feldkamp, D. Führer, M. Luster, T.J. Musholt, C. Spitzweg, M. Schott, Fine Needle Aspiration in the Investigation of Thyroid Nodules, Dtsch Arztebl Int 113(20) (2016) 353-9.

[36] A. Prete, P. Borges de Souza, S. Censi, M. Muzza, N. Nucci, M. Sponziello, Update on Fundamental Mechanisms of Thyroid Cancer, Front Endocrinol (Lausanne) 11 (2020) 102.

[37] E.D. Rossi, M. Papotti, W. Faquin, L.M. Larocca, L. Pantanowitz, The Diagnosis of Hyalinizing Trabecular Tumor: A Difficult and Controversial Thyroid Entity, Head Neck Pathol (2019).

[38] C.D. Seib, J.A. Sosa, Evolving Understanding of the Epidemiology of Thyroid Cancer, Endocrinol Metab Clin North Am 48(1) (2019) 23-35.

[39] T. Stokowy, B. Wojtas, B. Jarzab, K. Krohn, D. Fredman, H. Dralle, T. Musholt, S. Hauptmann, D. Lange, L. Hegedüs, R. Paschke, M. Eszlinger, Two-miRNA classifiers differentiate mutation-negative follicular thyroid carcinomas and follicular thyroid adenomas in fine needle aspirations with high specificity, Endocrine 54(2) (2016) 440-447.

[40] M. Toss, I. Miligy, K. Gorringe, K. Mittal, R. Aneja, I. Ellis, A. Green, E. Rakha, Prognostic significance of cathepsin V (CTSV/CTSL2) in breast ductal carcinoma in situ, J Clin Pathol 73(2) (2020) 76-82.

[41] M. Skrzypczak, A. Springwald, C. Lattrich, J. Häring, S. Schüler, O. Ortmann, O. Treeck, Expression of cysteine protease cathepsin L is increased in endometrial cancer and correlates with expression of growth regulatory genes, Cancer Invest 30(5) (2012) 398-403.

[42] J. Jing, S. Wang, J. Ma, L. Yu, H. Zhou, Elevated CTSL2 expression is associated with an adverse prognosis in hepatocellular carcinoma, Int J Clin Exp Pathol 11(8) (2018) 4035-4043.

[43] I. Santamaría, G. Velasco, M. Cazorla, A. Fueyo, E. Campo, C. López-Otín, Cathepsin L2, a novel human cysteine proteinase produced by breast and colorectal carcinomas, Cancer Res 58(8) (1998) 1624-30.

[44] M.M. Mohamed, B.F. Sloane, Cysteine cathepsins: multifunctional enzymes in cancer, Nat Rev Cancer 6(10) (2006) 764-75.

[45] M.S. Balda, K. Matter, Epithelial cell adhesion and the regulation of gene expression, Trends Cell Biol 13(6) (2003) 310-8.

[46] M. Saitoh, Involvement of partial EMT in cancer progression, J Biochem 164(4) (2018) 257-264.

[47] A. Satelli, S. Li, Vimentin in cancer and its potential as a molecular target for cancer therapy, Cell Mol Life Sci 68(18) (2011) 3033-46.

[48] V.N. Tzelepi, A.C. Tsamandas, H.D. Vlotinou, C.E. Vagianos, C.D. Scopa, Tight junctions in thyroid carcinogenesis: diverse expression of claudin-1, claudin-4, claudin-7 and occludin in thyroid neoplasms, Mod Pathol 21(1) (2008) 22-30.

[49] J. Kurebayashi, K. Tanaka, T. Otsuki, T. Moriya, H. Kunisue, M. Uno, H. Sonoo, All-trans-retinoic acid modulates expression levels of thyroglobulin and cytokines in a new human poorly differentiated papillary thyroid carcinoma cell line, KTC-1, J Clin Endocrinol Metab 85(8) (2000) 2889-96.

[50] T. Pilli, K.V. Prasad, S. Jayarama, F. Pacini, B.S. Prabhakar, Potential utility and limitations of thyroid cancer cell lines as models for studying thyroid cancer, Thyroid 19(12) (2009) 1333-42.

[51] C. Belgiovine, I. Chiodi, C. Mondello, Telomerase: cellular immortalization and neoplastic transformation. Multiple functions of a multifaceted complex, Cytogenet Genome Res 122(3-4) (2008) 255-62.

[52] T. Takenouchi, M. Yoshioka, N. Yamanaka, H. Kitani, Reversible conversion of epithelial and mesenchymal phenotypes in SV40 large T antigen-immortalized rat liver cell lines, Cell Biol Int Rep (2010) 17(1) (2010) e00001.

[53] K. Müntener, R. Zwicky, G. Csucs, J. Rohrer, A. Baici, Exon skipping of cathepsin B: mitochondrial targeting of a lysosomal peptidase provokes cell death, J Biol Chem 279(39) (2004) 41012-7.

[54] B.F. Sloane, J. Rozhin, K. Johnson, H. Taylor, J.D. Crissman, K.V. Honn, Cathepsin B: association with plasma membrane in metastatic tumors, Proc Natl Acad Sci U S A 83(8) (1986) 2483-7.

[55] M. Vizovišek, M. Fonović, B. Turk, Cysteine cathepsins in extracellular matrix remodeling: Extracellular matrix degradation and beyond, Matrix Biol 75-76 (2019) 141-159.

[56] L.J. Burton, J. Dougan, J. Jones, B.N. Smith, D. Randle, V. Henderson, V.A. Odero-Marah, Targeting the Nuclear Cathepsin L CCAAT Displacement Protein/Cut Homeobox Transcription Factor-Epithelial Mesenchymal Transition Pathway in Prostate and Breast Cancer Cells with the Z-FY-CHO Inhibitor, Mol Cell Biol 37(5) (2017).

[57] P.C. Ong, S. McGowan, M.C. Pearce, J.A. Irving, W.T. Kan, S.A. Grigoryev, B. Turk, G.A. Silverman, K. Brix, S.P. Bottomley, J.C. Whisstock, R.N. Pike, DNA accelerates the inhibition of human cathepsin V by serpins, J Biol Chem 282(51) (2007) 36980-6.

[58] J.N. Marhefka, R.A. Abbud-Antaki, Validation of the Cancer BioChip System as a 3D siRNA screening tool for breast cancer targets, PLoS One 7(9) (2012) e46086.

[59] C.H. Wong, Z. Wu, Q. Yu, CTSL2 is a pro-apoptotic target of E2F1 and a modulator of histone deacetylase inhibitor and DNA damage-induced apoptosis, Oncogene 33(10) (2014) 1249-57.

[60] T.C. Hallstrom, S. Mori, J.R. Nevins, An E2F1-dependent gene expression program that determines the balance between proliferation and cell death, Cancer Cell 13(1) (2008) 11-22.

[61] S. Inoshita, Y. Terada, O. Nakashima, M. Kuwahara, S. Sasaki, F. Marumo, Regulation of the G1/S transition phase in mesangial cells by E2F1, Kidney Int 56(4) (1999) 1238-41.

[62] D.G. Johnson, W.D. Cress, L. Jakoi, J.R. Nevins, Oncogenic capacity of the E2F1 gene, Proc Natl Acad Sci U S A 91(26) (1994) 12823-7.

[63] I. Molina-Privado, M. Rodríguez-Martínez, P. Rebollo, D. Martín-Pérez, M.J. Artiga, J. Menárguez, E.K. Flemington, M.A. Piris, M.R. Campanero, E2F1 expression is deregulated and plays an oncogenic role in sporadic Burkitt's lymphoma, Cancer Res 69(9) (2009) 4052-8.

[64] P.K. Tsantoulis, V.G. Gorgoulis, Involvement of E2F transcription factor family in cancer, Eur J Cancer 41(16) (2005) 2403-14.

[65] M. Onda, H. Nagai, A. Yoshida, S. Miyamoto, S.I. Asaka, J. Akaishi, K. Takatsu, M. Nagahama, K. Ito, K. Shimizu, M. Emi, Up-regulation of transcriptional factor E2F1 in papillary and anaplastic thyroid cancers, J Hum Genet 49(6) (2004) 312-318.

Supplemental Material

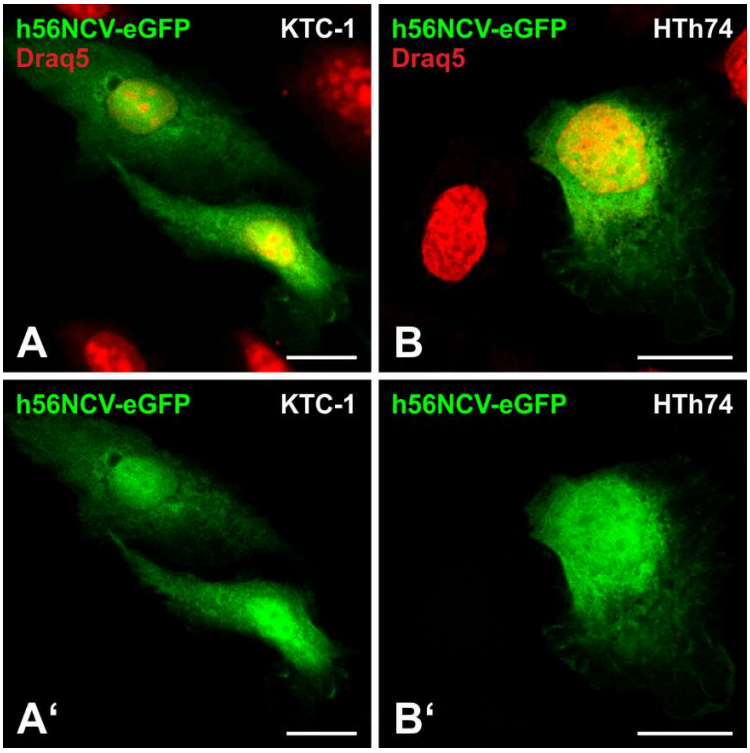

Supplementary Figure 1: Localization of eGFP-tagged N-terminally truncated cathepsin V chimeras in thyroid carcinoma cells. Single channel and corresponding merged fluorescence micrographs of KTC-1 (A and A') and HTh74 cells (B and B') after transfection with the plasmid coding for eGFP-tagged N-terminally truncated cathepsin V (h56NCV-eGFP, green signals) and counter-staining of nuclear DNA with Draq5 (red signals). The chimeric protein h56NCV-eGFP was localized to the cytosol and nuclei of transfected cells, only (A and B). Scale bars represent 20 µm.